Energy Conversion and Management 266 (2022) 115783

Contents lists available at ScienceDirect

Energy Conversion and Management

journal homepage: www.elsevier.com/locate/enconman

# Performance of binary zeotropic mixtures in organic Rankine cycles (ORCs)

Mina Shahrooz [a,*], Per Lundqvist [a], Petter Nekså [b]

[a] Department of Energy Technology, KTH Royal Institute of Technology, SE-100 44, Stockholm, Sweden
[b] SINTEF Energy Research and Norwegian University of Science and Technology, 7034 Trondheim, Norway

ARTICLE INFO

*Keywords:*
ORC
Rankine cycle
Zeotropic mixture
Binary mixture
Natural fluids
Waste heat recovery

ABSTRACT

Compared to pure fluids, zeotropic mixtures have the potential to lower the irreversibilities in low temperature Rankine cycles by better temperature profile matching of the working fluid with the heat source/sink. However, having a gliding temperature does not guarantee performance boost over pure fluids, as many factors influence the exergy efficiency of the cycle. In this study, 25 pure fluids and 104 binary mixtures of natural working fluids are analyzed in subcritical ORCs with heat source temperature range of 125–300 °C and different condensing conditions and the results are investigated within two frameworks: (1) comparing the mixtures to their pure constituents, (2) comparing the mixtures to the best performing pure fluid. In one behavior type, the performance of the mixture falls between the performance of its pure constituents for all evaporator pressure range, and the mixture provides no benefit. However, some mixtures could provide performance boost in a specific evaporator range. Therefore, the maximum allowable evaporator pressure plays an important role in the performance comparison of zeotropic mixtures to their pure constituents. Mixtures which outperform their pure constituents in the first perspective, are further analyzed in the second perspective. Finally, a screening method is presented to map the binary mixtures with performance boost compared to their pure constituents and high absolute exergy efficiency. This method is based on the key thermophysical properties of the fluids including critical temperature and normal boiling point, as well as working conditions such as heat source and heat sink temperature and PPTD in the evaporator and the condenser.

## 1. Introduction

Organic Rankine Cycle (ORC) is a prominent solution for power generation with low-to-medium temperature heat sources such as waste heat recovery applications [1–3]. In this cycle, heat is extracted from the heat source and fed to the pressurized working fluid, which expands later in the expander and generates power. The fluid is later condensed back to the liquid state.

The choice of the optimal working fluid is an important design parameter in ORCs. Working conditions such as heat source and heat sink temperatures as well as the performance criteria of the cycle affect the optimal working fluids [4]. Many studies have focused on the selection criteria of working fluids to maximize their performance in ORCs. These criteria include different thermophysical properties of the fluids and characteristics of the heat source/sink such as critical temperature, critical pressure, normal boiling point, specific heat capacity, latent heat and other factors. Critical temperature is the most common used property among these parameters to identify the fluids with expected maximum performance under specific working conditions [5–12]. Haervig et al. [8] analyzed 26 pure fluids and 3 mixtures at heat source temperature range of 50–280 °C and found that the optimal critical temperature of the fluid should be 30–50 K less than the heat source inlet temperature to maximize net power. Ayachi et al. [12] found the optimal critical temperature of the fluid to be 33 K less than the heat source temperature to maximize exergy efficiency. On the other hand, several papers have focused on presenting fitting expressions to relate the performance of the cycle to the working conditions and key thermophysical properties of the fluids [10,13–16]. These parameters mostly include heat source temperature, evaporation temperature and Pinch Point Temperature Difference (PPTD). Zhai et al. proposed a linear correlation for optimal critical temperature based on the heat source inlet temperature [10].

Due to the low quality of the heat, the efficiency of ORCs is usually low compared to cycles with high grade heat sources [5]. Therefore, novel ideas are introduced and investigated to enhance the performance ORCs. Using zeotropic mixtures instead of pure fluids, is one possibility to boost the performance of ORCs [17–23]. Zeotropic mixtures exhibit temperature change during the phase change process, which could possibly reduce the irreversibility in the condenser and/or the

* Corresponding author.
*E-mail addresses:* minash@kth.se (M. Shahrooz), per.lundqvist@energy.kth.se (P. Lundqvist), petter.neksa@sintef.no (P. Nekså).

https://doi.org/10.1016/j.enconman.2022.115783
Received 29 October 2021; Received in revised form 14 May 2022; Accepted 16 May 2022
Available online 1 June 2022

**Nomenclature**

| | |
|---|---|
| $\dot{E}$ | Exergy (kW) |
| $\dot{I}$ | Irreversibility (kW) |
| $P_1$ | Condensing pressure (kPa) |
| $\dot{Q}_{evap}$ | Extracted heat rate in the evaporator (kW) |
| $T_1$ | Condensing temperature (°C), bubble point in condenser for mixtures (°C) |
| $T_b$ | Normal boiling point (°C) |
| $T_c$ | Critical temperature (°C) |
| $T_c^*$ | Border of critical temperature, which divides fluids based on $T_b$ and $T_{cond,min}$ (°C) |
| $T_{cond,min}$ | Minimum condensing temperature (°C) |
| $T_{h,eff}$ | Effective heat source temperature (°C) |
| $\dot{W}_{net}$ | Net power (kW) |

*Greek symbols*

| | |
|---|---|
| $\eta_{II}$ | Exergy efficiency (-) |
| $\eta_{th}$ | Thermal efficiency (-) |
| $\min\Delta T_c$ | Minimum temperature rise in the heat sink (K)(in the phase change part of the condenser) |

*Subscripts*

| | |
|---|---|
| 1 | Pump inlet/condenser outlet |
| 2 | Pump outlet/evaporator inlet |
| 3 | Evaporator outlet/expander inlet |
| 4 | Expander outlet/condenser inlet |
| c | Heat sink |
| cond. | Condenser |
| evap. | Evaporator |
| exp. | Expander |
| h | Heat source |
| in | Inlet |
| out | Outlet |
| p | Pump |
| tot. | Total |

*Abbreviations*

| | |
|---|---|
| EoS | Equations of State |
| LLE | Liquid-Liquid Equilibrium |
| min. | Minimum |
| ORC | Organic Rankine Cycle |
| PPTD | Pinch Point Temperature Difference (K) |
| VLE | Vapor-Liquid Equilibrium |

evaporator and therefore increase the exergy efficiency and consequently net power [21].

Different investigations have been carried out to assess the performance of the mixtures compared to pure fluids and if possible, propose mixture selection criteria. Haervig et al. also proposed the same criterion for mixture critical temperature to be 30–50 K less than the heat source inlet temperature together with condenser glide close to temperature rise in the heat sink [8]. Miao et al. proposed selection criteria for zeotropic mixtures in subcritical cycles, identifying suitable range for critical temperature as well as condenser glide matching by analyzing 11 mixtures [18]. Lecompte et al. [22] analyzed 8 mixtures with heat source temperature of 120–160 ℃ in subcritical cycles and found that the improvement in exergy efficiency of the mixtures is between 7.1 and 14.2% compared to pure fluids. Deethayat et al. [23] investigated the performance of 6 mixtures and developed an empirical correlation to estimate the cycle efficiency for a specific condensing and evaporating temperature. Moreover, other studies focused on mixture composition adjustments during operation [24] and effects of restrictive conditions on the performance of zeotropic mixtures [25].

Modi et al. [26] have done extensive review on the research on zeotropic mixtures in ORCs and presented the results in different application sectors. Despite many research efforts to optimize ORCs with zeotropic mixtures and identify the suitable working fluids, there is no unified conclusion, and guidelines to select mixture working fluids are missing. This is mainly due to the different boundary conditions, assumptions, optimization objectives and initial working fluid candidates in various researches [5].

In this study, 25 pure fluids and 104 binary mixtures of natural working fluids are analyzed in subcritical ORCs with heat source temperature range of 125–300 ℃. The performance of the cycle is evaluated by exergy efficiency and the results are investigated within two frameworks: (1) comparing the mixtures to their pure constituents, (2) comparing the mixtures to the best performing pure fluid. Mixtures which outperform their pure constituents in the first perspective, are further analyzed in the second perspective. Finally, a screening method is presented to map the binary mixtures with performance boost compared to pure constituents and high absolute exergy efficiency. This method is based on the key thermophysical properties of the fluids including critical temperature and normal boiling point, as well as working conditions such as heat source and heat sink temperature and PPTD in the evaporator and the condenser.

Although the mixtures are evaluated by their thermal performance, other factors such as heat exchanger and expander design and costs, affect the choice of appropriate working fluids and mixtures. It is important to note that this paper presents preliminary screening method for mixtures to be used in further investigations. Taking into account the number of possible binary mixtures and compositions, it is not feasible to evaluate the detailed performance and design of all the possible cases, including all the factors. If a mixture with its optimum heat exchanger and expander design does not have improved exergy efficiency compared to its pure constituents, introducing factors such as costs and detailed component design will not improve the performance of the mixture. This is due to the challenges associated with zeotropic mixtures compared to pure fluids. Therefore, this paper could help to reduce the number of possible mixture combinations for evaluation. Screened mixtures can be evaluated in detail, in the next phase considering different component design and thermo-economic performance.

## 2. ORC description

Fig. 1 shows the basic layout of an ORC with 4 components [17]. By

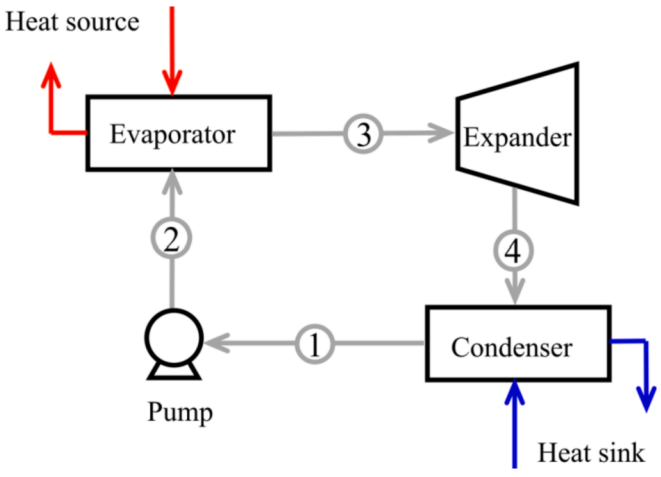


**Fig. 1.** Basic layout of an ORC.

applying exergy balance to the cycle components, heat source and the heat sink, described by [27]:

$$\dot{E}_{h,in} + \dot{E}_{c,in} = \dot{W}_{net} + \dot{I}_{tot.} \quad (1)$$

Where:

$$\dot{I}_{tot.} = \sum \dot{I} = \dot{I}_p + \dot{I}_{exp.} + \dot{I}_{evap.} + \dot{I}_{cond.} + \dot{I}_h + \dot{I}_c \quad (2)$$

The term $\dot{I}_{tot.}$ is the summation of all the irreversibilities in the system. Irreversibility in the pump and the expander are related to their isentropic efficiencies. $\dot{I}_h$ refers to the unextracted exergy of the heat source, which is not used, and $\dot{I}_c$ refers to the exergy of the heat sink leaving the system. If the inlet characteristics of the heat sink are the same as the reference point, $\dot{E}_{c,in}$ will be equal to zero. With definition of exergy efficiency as:

$$\eta_{II} = \frac{\dot{W}_{net}}{\dot{E}_{h,in}} \quad (3)$$

We will have:

$$\eta_{II} + \frac{\dot{I}_{tot.}}{\dot{E}_{h,in}} = 1 \quad (4)$$

Therefore, for a given heat source (fixed $\dot{E}_{h,in}$), maximizing exergy efficiency means maximizing net power and minimizing total irreversibilities in the system.

Fig. 2 shows temperature vs. transferred heat in a subcritical ORC with pure fluid. For pure fluids, the location of the pinch point in the evaporator could vary between the evaporator inlet to the saturated liquid, while the location of the pinch point in the condenser is at saturated vapor. PPTD affects the design of the heat exchangers and exergy loss. However, its effects on net power could be combined with other parameters in the cycle. In the evaporator, the effects of the heat source inlet temperature and PPTD in the evaporator could be combined into effective heat source temperature, defined as:

$$T_{h,eff} = T_{h,in} - PPTD_{evap.} \quad (5)$$

In the condenser, the effects of the heat sink inlet temperature, the PPTD in the condenser and the minimum temperature rise in the heat sink (in the phase change part of the condenser) could be combined into minimum condensing temperature, defined as:

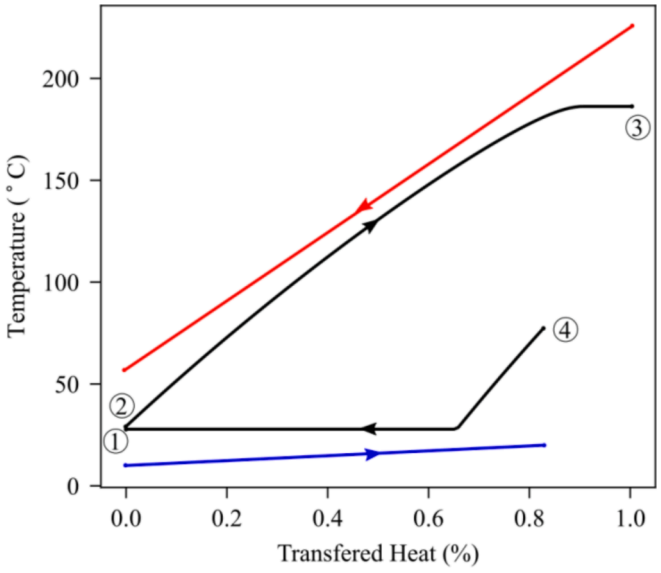


**Fig. 2.** Temperature vs. transferred heat rate diagram in an ORC.

$$T_{cond,min} = T_{c,in} + PPTD_{cond.} + \min\Delta T_c \quad (6)$$

Therefore, the changes in these three variables could be summarized into changes in minimum condensing temperature. Cases with the same $T_{h,eff}$ and $T_{cond,min}$ have the same pinch point location in the evaporator and same behavior trends in net power and exergy efficiency for a specific working fluid. The values of net power will be the same. However, exergy efficiency values will differ, as it is defined based on the heat source inlet temperature and ambient temperature. The reason to assume a value for minimum heat sink temperature rise in the phase change part of the condenser is to eliminate the effects of superheat degree at expander outlet on the minimum condensing temperature and compare fluids based on the same minimum condensing temperature.

As the glide decreases with pressure, the glide in the evaporator will be typically less than the glide in the condenser. Besides, the temperature change in the heat source is much higher than the temperature change in the heat sink. Therefore, many studies dealing with zeotropic mixtures, focus on the temperature profile matching in the condenser and ways to reduce irreversibility in the condenser [28]. However, optimum glide matching does not result in optimal performance [29]. This is due to the effects of $\dot{I}_{tot.}$ on exergy efficiency (Eq. (4)). Although temperature profile matching could result in reduced $\dot{I}_{cond.}$, the overall performance of the cycle depends on $\dot{I}_{tot.}$ and how the other sources of the irreversibility change in the cycle. Therefore, glide matching in the condenser does not necessarily guarantee increased exergy efficiency. This argument is discussed in detail in section 5.2.1.

While wet mixtures are avoided due to high required superheat in the expander [30], there is a possibility to minimize the superheat in the expander and match with the isentropic efficiency of the expander [31]. Therefore, wet mixtures should not be excluded from optimizations.

## 3. Theory of mixtures

Mixtures of two or more components are categorized into two major groups, based on their behavior during the evaporation/condensation phase change process: *azeotropic* and *zeotropic*. In azeotropic mixtures, the temperature is constant during the phase change and the mixture acts like a pure fluid, evaporating and condensing at the same temperature, at a specific pressure and composition mix(s). These points are azeotropes and the mixtures which form them, are called azeotropic mixtures. On the other hand, the mixtures which do not form any azeotropes, are called zeotropic. These mixtures exhibit variable temperature profile during the phase change process. The term 'glide' is commonly used to point to the temperature difference between dew and bubble temperature at a specific pressure [4,32,33].

Therefore, the definition of zeotropic mixtures is intertwined with the identification of the azeotropes. Absence of azeotropes confirms zeotropic type. Vapor-Liquid Equilibrium (VLE) data is used to identify the type of the mixtures. This data is represented graphically as temperature-composition graphs, where bubble and dew temperatures are plotted vs. composition at a specific pressure (isobar line). Pressure-composition graphs could also represent VLE data at a specific temperature (isothermal line).

### 3.1. Binary mixtures

Fig. 3 presents the most common types of binary mixtures at constant pressure, where the mixture at any composition range lies in the subcritical region. In these mixtures, the liquid phase is stable at a given pressure regardless of the composition or temperature. Therefore, the mixture does not exhibit Liquid-Liquid Equilibrium (LLE) [33,34]. In case the pressure is higher than the critical pressure for a composition range, the curves become partial and do not cover the whole composition range [34].

In zeotropic mixtures, bubble and dew temperature change

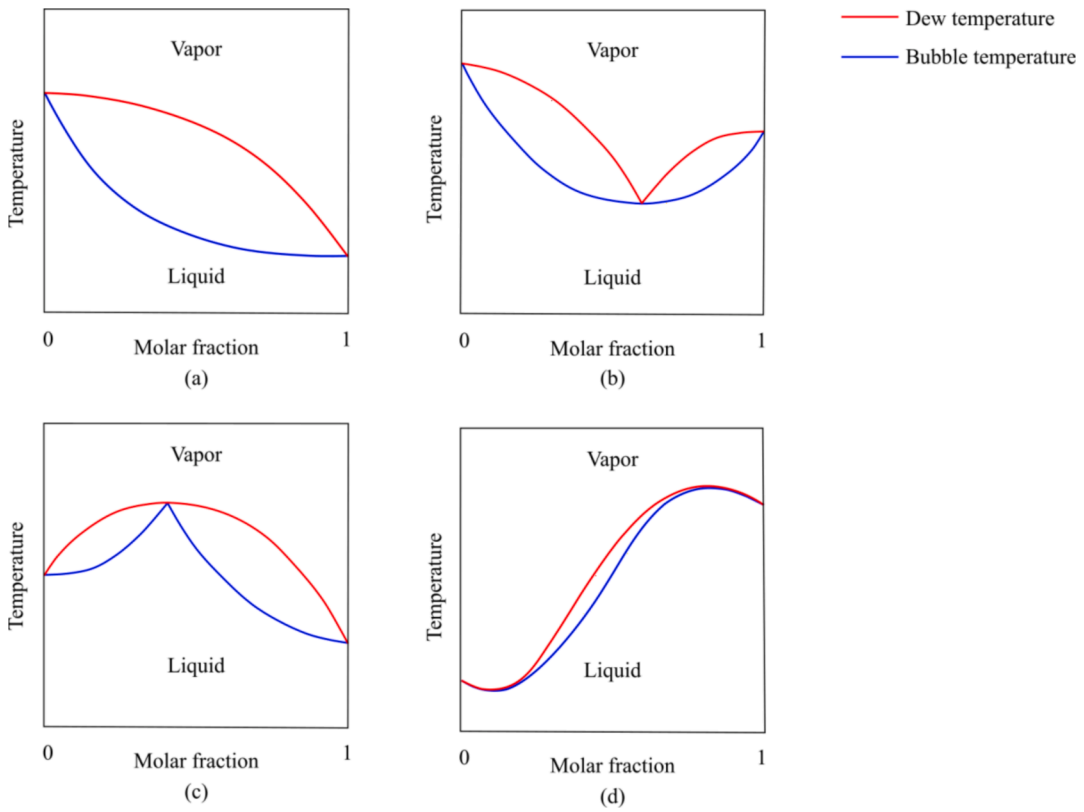


**Fig. 3.** Most common binary mixtures: (a) zeotropic, (b) minimum-boiling azeotropic, (c) maximum-boiling azeotropic [32], (d) double-azeotropic [36].

monotonically from one pure fluid to the other one, maintaining a positive glide (Fig. 3a). However, in azeotropic mixtures, these curves intersect with each other once (where glide becomes zero), and in rare cases twice. Most common azeotropic mixture types are minimum-boiling and maximum-boiling, shown in Fig. 3b, and c respectively. In the minimum-boiling type, the boiling temperature of the azeotrope is lower than the boiling temperature of both its pure constituents, while in maximum-boiling type, boiling temperature of the azeotrope is higher than both its pure constituents [32,35]. Most discovered azeotropes are minimum-boiling type [36]. There is also a rare type, where two stable azeotropes at different compositions exist at a given pressure, one local minimum and one local maximum azeotrope (Fig. 3d) [36]. Mixture of benzene/hexafluorobenzene is an example of double-azeotropic type [37].

Pressure affects the glide and the composition of the azeotrope point if it exists [38]. Fig. 4 shows glide vs. composition for both zeotropic (butane/pentane) and azeotropic (acetone/hexane) mixtures at different pressures. The composition of the azeotrope point changes with pressure (Fig. 4b). In binary zeotropic mixtures, glide decreases as the pressure increases for any composition mix (Fig. 4a). Therefore, glide in condenser is higher than the glide in the evaporator. This fact also applies to azeotropic mixtures in regions far from the azeotrope point. Around the azeotrope point, there is a region that glide increases with pressure.

There is also another sub-group of mixtures which have variable temperature during the phase change process, but the glide is so small, usually between 0.2 and 0.6 K that it is negligible. This behavior includes both azeotropic and zeotropic mixtures. This sub-category is called *Near-Azeotropic*. As the maximum glide decreases with pressure, minimum operating pressure plays an important role in identifying a mixture as near-azeotropic. In this paper, the mixtures whose maximum glide at minimum pressure is less than 1 K, are categorized as near-azeotropic. For example, a mixture of *trans*-butene/*cis*-butene behaves as Fig. 3d. However, the maximum glide at pressure of 101.3 kPa is only

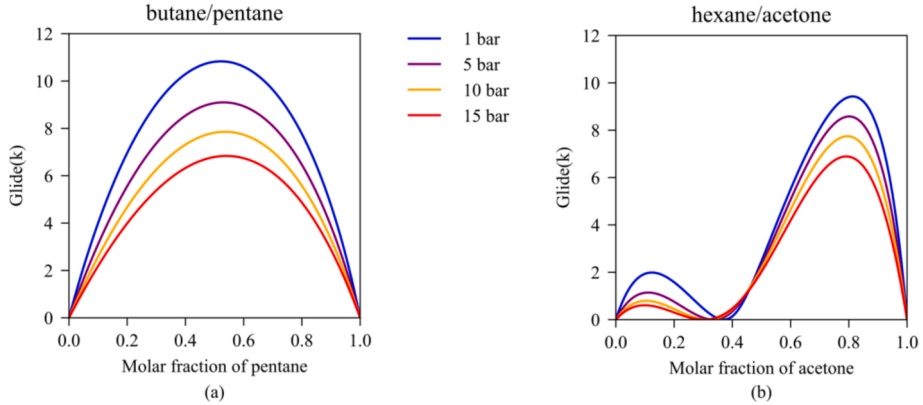


**Fig. 4.** Effect of pressure on: (a) zeotropic mixture of butane/pentane, (b) azeotropic mixture of hexane/acetone.

0.37 K which is considered near-azeotropic.

Depending on the lowest and highest operating pressure range for a mixture, there is a range of composition where an azeotropic mixture forms an azeotrope. Outside this region, the mixture has a zeotropic behavior. For instance, a mixture of hexane/acetone in the pressure range of 1–15 bar with acetone molar fraction of over 0.5, has a zeotropic behavior (Fig. 4b).

## 4. Assumptions and hypotheses

In this study, pure natural fluids provided in REFPROP 10.0 [39] were analyzed with custom code in python using Numpy [40], Pandas [41] and Scipy [42] packages. Visualization was done through Matplotlib [43] and Seaborn [44]. Only natural fluids with critical temperature up to 240 ℃ were selected for further investigation. Exergy efficiency of the fluids with higher critical temperature, drops significantly due to high normal boiling point which increases condensing temperature levels. This reason is thoroughly explained in section 5.1.1. Then, binary mixtures of these fluids whose interaction parameters were available in REFPROP, were analyzed. Thermodynamic modelling of the cycles was based on the equations presented in [27].

The mixtures were studied in subcritical cycles. Heat source inlet temperature varied between 125 and 300 ℃ with minimum PPTD of 10 K in the evaporator. The expender inlet was set to saturated vapor. The pump and the expander were modeled with fixed isentropic efficiencies. Minimum condensing pressure was set to 101.3 kPa to avoid any air suction to the system in case of leakage. For condensing conditions, 4 cases were defined based on the minimum condensing temperature for pure fluids (25, 40 ℃) and minimum temperature rise in the heat sink (5, 10 K). Minimum condensing temperature takes into account changes in the ambient temperature, PPTD in the condenser as well as minimum heat sink temperature rise. Minimum temperature rise in the heat sink shows how much the glide in the condenser could be used to lower the bubble temperature in the mixture. This is explained in detail in section 5.1.1. Case 1 is considered as the main reference case and results are primarily presented for this case. The effects of changing minimum condensing temperature and minimum temperature rise are also explained. Adding superheat to the expander inlet, decreases mass flow rate of the working fluid and consequently decrease exergy efficiency of the cycle [45]. Therefore, no superheat was added to the expander inlet.

Table 1 summarizes the details of different cases.

Table 2 summarizes all the assumptions and hypotheses used in this paper.

### 4.1. Studied pure fluids and mixtures

Table 3 represents the list of pure fluids in this study, as well as properties such as critical temperature and pressure, normal boiling point, molecular weight and group of the fluid. Fluids are sorted based on their critical temperature in ascending order.

Fig. 5 shows all the possible binary compositions of the studied pure fluids. All the fluids are organized in ascending order of their critical temperature. The horizontal axis shows the fluid with lower critical temperature ($T_{c,1}$) and the vertical axis represents the fluid with higher critical temperature ($T_{c,2}$). In this table, the pairs whose interaction parameter are not available are marked as well as different types of mixtures (azeotropic, zeotropic, near-azeotropic) for the pairs whose interaction parameters are available. Mixtures are categorized as near-azeotropic based on their maximum glide at minimum operating pressure below 1 K. For near-azeotropic mixtures, it is also revealed if the mixture belongs to zeotropic or azeotropic main category. Cells with white color correspond to mixtures of ammonia whose interaction parameters are available, but REFPROP models need revision to have more accurate calculations. Many ammonia mixtures exhibit LLE [46] while the present version of REFPROP is limited to VLE and does not address other complex forms of phase equilibrium [39]. Therefore, these mixtures are not included in the present study.

The performance of these mixtures is studied and compared to pure fluids in order to assess the potential of zeotropic mixtures and map the pairs with boosted performance.

**Table 1**
List of cases defined based on condensing conditions.

| Specifications of each case | Case 1 (ref.) | Case 2 | Case 3 | Case 4 |
|---|---|---|---|---|
| Ambient and heat sink inlet temperature (°C) | 10 | 25 | 10 | 25 |
| **Min. temperature rise in the heat sink (K)** (in the phase change part of the condenser) | **5** | **5** | **10** | **10** |
| **Min. condensing temperature for pure fluids** (°C) | **25** | **40** | **25** | **40** |
| Min. mixture bubble point (°C) | 20 | 35 | 15 | 30 |
| Min. mixture dew point (°C) | 25 | 40 | 25 | 40 |
| Min. PPTD in the condenser (k) | 10 | 10 | 5 | 5 |

**Table 2**
List of parameters in the optimizations.

| Parameter | Value |
|---|---|
| Heat source | Air with inlet temperature 125–300 °C |
| Heat sink | River or sea water with inlet temperature 10–25 °C |
| Ambient temperature and pressure | 10–25 °C, 101.325 kPa |
| Pump isentropic efficiency | 0.9 |
| Expander isentropic efficiency | 0.8 |
| Min. condensing pressure | 101.325 kPa |
| Min. condensing temperature | 25–40 °C (pure fluids and mixture dew point), 20–30 °C (mixture bubble point) |
| Min. temperature rise in the heat sink | 5–10 K |
| Min. PPTD in the evaporator | 10 K |
| Min. PPTD in the condenser | 5–10 K |

### 4.2. Validation

In this project, only the mixtures whose interaction parameters were available in REFPROP, were investigated. Binary interaction parameters represent the molecular interaction between different components in the mixture. They are used in the Equations of State (EoS) to calculate the thermophysical properties of mixtures [47]. These parameters are obtained by fitting experimental data sources described by Bell et al. [48]. Mixtures whose interaction parameters were estimated, were not included in the study. Furthermore, the results obtained from REFPROP were compared to experimental study of zeotropic mixture by Wang et al. [49]. In this paper, an experimental study on the performance of a small-scale ORC was conducted using zeotropic mixture of isobutane/isopentane.

The pump work and the generator efficiency were not exactly reported in this paper. The pump work was reported to be within the range of 0.04–0.1 of expander work. Therefore, assuming pump work to be 7% of expander work and neglecting generator losses, Fig. 6 shows net power vs. composition in mixture of isobutane/isopentane, for experimental data and calculated by REFPROP.

As shown in this figure, both REFPROP and the experimental study follow the same behavior trend in the electrical power for different molar composition in the mixture of isobutane/isopentane. However, the exact values differ which is due to the non-availability of the pump work values and generator efficiency. The mean relative deviation is 6.9%.

## 5. Results and discussion

In this section, the results of the study are presented for binary

**Table 3**
List of pure fluids considered in the design of binary mixtures.

| No. | Name of fluid | Group | Crit. temp. (°C) | Crit. pressure (bar) | Normal boiling point (°C) | Molecular weight (gr/mol) |
|---|---|---|---|---|---|---|
| 1 | methane | alkane | −82.6 | 46.0 | −161.5 | 16.0 |
| 2 | ethylene | alkene | 9.2 | 50.4 | −103.8 | 28.1 |
| 3 | carbon dioxide | — | 31.0 | 73.8 | — | 44.0 |
| 4 | ethane | alkane | 32.2 | 48.7 | −88.6 | 30.1 |
| 5 | propylene | alkene | 91.1 | 45.6 | −47.6 | 42.1 |
| 6 | propane | alkane | 96.7 | 42.5 | −42.1 | 44.1 |
| 7 | carbonyl sulfide | — | 105.6 | 63.7 | −50.2 | 60.1 |
| 8 | cyclopropane | cycloalkyne | 125.2 | 55.8 | −31.5 | 42.1 |
| 9 | dimethylether | ether | 127.2 | 53.4 | −24.8 | 46.1 |
| 10 | propyne | alkyne | 129.2 | 56.3 | −25.1 | 40.1 |
| 11 | ammonia | — | 132.3 | 113.3 | −33.3 | 17.0 |
| 12 | isobutane | alkane | 134.7 | 36.3 | −11.8 | 58.1 |
| 13 | isobutene | alkene | 144.9 | 40.1 | −7.0 | 56.1 |
| 14 | butene | alkene | 146.1 | 40.1 | −6.3 | 56.1 |
| 15 | butane | alkane | 152.0 | 38.0 | −0.5 | 58.1 |
| 16 | *trans*-butene | alkene | 155.5 | 40.3 | 0.9 | 56.1 |
| 17 | neopentane | alkane | 160.6 | 32.0 | 9.5 | 72.1 |
| 18 | *cis*-butene | alkene | 162.6 | 42.3 | 3.7 | 56.1 |
| 19 | isopentane | alkane | 187.2 | 33.8 | 27.8 | 72.1 |
| 20 | diethyl ether | ether | 193.6 | 36.4 | 34.4 | 74.1 |
| 21 | pentane | alkane | 196.6 | 33.7 | 36.1 | 72.1 |
| 22 | isohexane | alkane | 224.6 | 30.4 | 60.2 | 86.2 |
| 23 | hexane | alkane | 234.7 | 30.3 | 68.7 | 86.2 |
| 24 | acetone | ketone | 235.0 | 47.0 | 56.1 | 58.1 |
| 25 | cyclopentane | cycloalkyne | 238.6 | 45.7 | 49.2 | 70.1 |

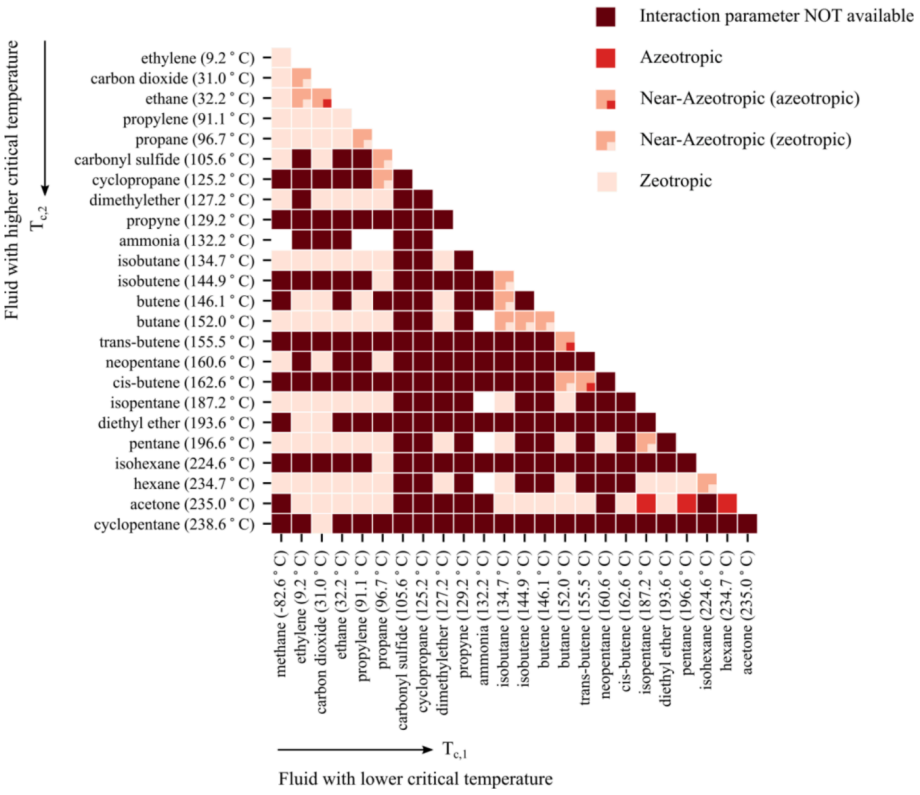


**Fig. 5.** Combination of binary mixtures with critical temperature up to 240 ℃ with their mixture type categories.

mixtures. In section important factors affecting the behavior of the mixtures are discussed, and then in section 5.2 performance comparison between binary mixtures and pure fluids is explained in detail.

There are two major factors which determine how a binary mixture would behave compared to its pure constituents.

### 5.1. Condensing conditions

Condensing conditions play an important role in the mixture's behavior compared to its pure constituents. As mentioned in section 4, working fluids should satisfy both minimum condensing pressure (101.325 kPa) and temperature (25, 40 °C depending on the case). Therefore, for fluids whose normal boiling point is below the minimum

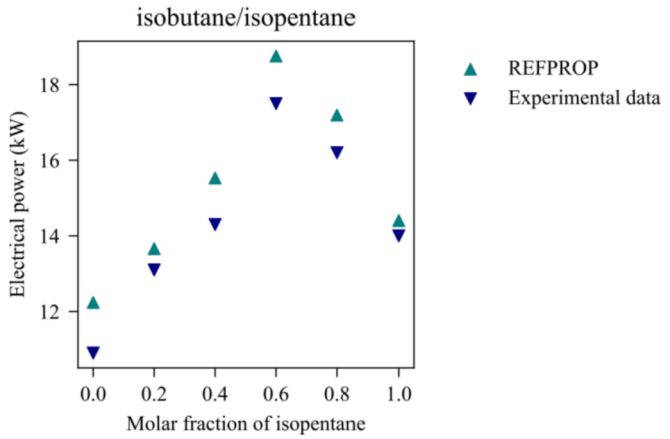


**Fig. 6.** validation for electrical power vs. composition for mixture of isobutane/isopentane, by REFPPROP (assuming 100% generator efficiency) and experimental data from Wang et al. [49], with mean relative deviation of 6.9%.

condensing temperature ($T_b < T_{cond,min}$), the temperature rule is dominant ($T_1 = T_{cond,min}$). Otherwise, the pressure rule applies ($P_1 = 101.3kPa$, $T_1 = T_b$).

Fig. 7 shows normal boiling point of pure natural fluids, available in REFPROP. Generally, normal boiling point increases with critical temperature. However, this change is not monotonic. Varshni [50] investigated the relationship between critical temperature and normal boiling point of organic compounds and showed that a simple relation as $1/T_c[K] = \alpha/T_b[K] + \beta$ is valid for many organic series where $\alpha > 0$ and $\beta > 0$ are constants for that specific organic group. Therefore, the changes of normal boiling temperature vs. critical temperature is not monotonic considering all organic groups as well as inorganic fluids.

For fluids with critical temperature above 240 ℃, normal boiling point increases significantly, resulting in low exergy efficiency values. Therefore, those fluids were excluded in the study and only pure fluids with critical temperature up to 240 ℃, present in Table 3 were further analyzed.

Fig. 8 presents the cases with different minimum condensing conditions. For the cases where $T_{cond,min} = 25\ °C$, there is a clear border at $T_c = 175\ °C$ which divides the fluids based on the condensing conditions (Fig. 8a). Fluids with $T_c < 175\ °C$, have normal boiling point below 25 °C and fluids with $T_c > 175\ °C$, have higher normal boiling point than 25 °C. For the case of $T_{cond,min} = 40\ °C$, this border is at 210 °C (Fig. 8c). This criterion is based on normal boiling point, rather than critical

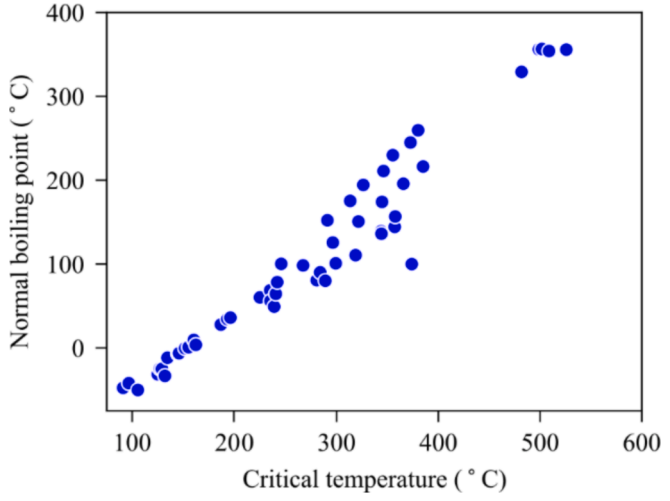


**Fig. 7.** Normal boiling point vs. critical temperature for pure natural fluids present in REFPROP.

temperature. For example, if the minimum condensing temperature was 50 °C, there was no specific border of critical temperature which could divide the list of fluids into two groups with normal boiling temperature below and above 50 °C. Instead, fluids would be categorized based on their normal boiling point either below or above minimum condensing temperature: $T_b < T_{cond,min}$ or $T_b > T_{cond,min}$.

Depending on the condensing conditions, the table in Fig. 5 could be divided into 3 regions of:

$T_{b,1}$, $T_{b,2} < T_{cond,min}$, $T_{b,1} < T_{cond,min} < T_{b,2}$, $T_{cond,min} < T_{b,1}$, $T_{b,2}$. Fig. 8b and Fig. 8d show region division for minimum condensing temperature of 25 °C and 40 °C, respectively. These regions are important in the mixture's behavior compared to its pure constituents. The red region marks the mixtures where the pressure rule applies to both fluids (the normal boiling point of pure constituents is higher than minimum condensing temperature). By increasing the minimum condensing temperature, the red region becomes smaller.

An important benefit of zeotropic mixtures is the possibility to lower the bubble temperature in the condenser ($T_1$) due to its glide. Fig. 9 shows how the bubble point in the condenser could be lowered for a zeotropic mixture (Fig. 9b) compared to a pure fluid (Fig. 9a). In pure fluid, the pinch point in the condenser is located at saturated vapor. On the other hand, in zeotropic mixtures, bubble point in the condenser could be reduced down to a temperature where pinch point occurs at saturated liquid. This is the minimum possible temperature for bubble point of a zeotropic mixture. This is where the effects of minimum temperature rise in the heat sink (5, 10 K) come into play. For cases with greater $\min\Delta T_c$ (10 K), bubble point in the condenser has more potential to further decrease compared to the case with lower $\min\Delta T_c$ (5 K). It only applies to mixtures whose glide in the condenser is higher than 5 K. Otherwise, $\min\Delta T_c$ does not affect the mixture.

The value of ($T_{c,in} + PPTD_{cond.}$) is the minimum possible value for the bubble temperature of mixture in the condenser. However, it might push the heat sink outlet temperature to a lower value than its minimum (dashed curves in Fig. 9c) and increase the needed heat sink mass flow rate significantly. Therefore, bubble temperature in the condenser should be increased to meet the criteria for minimum heat sink temperature (solid curves in Fig. 9c). In this case, pinch point in the condenser is in 2-phase region. Pinch point analysis method presented by Kim et al. [51] is used to calculate the pinch point location and heat sink outlet temperature and update bubble temperature in the condenser accordingly with this method, if needed. This method is also used to obtain heat source outlet temperature and pinch point location in the evaporator.

If the pressure rule applies to both fluids (red region in Fig. 8b and d), bubble point in the condenser could not decrease due to the minimum pressure limitation. Fig. 10 shows how the condenser bubble temperature could change for binary mixtures in different regions of Fig. 8b for the reference case ($T_{cond,min} = 25\ °C$, $\min\Delta T_c = 5K$).

If the critical temperature of at least one fluid is below 175 ℃, condenser bubble temperature could decrease compared to pure fluids, down to 20 ℃ which is the minimum possible bubble point in the condenser for case 1 (Fig. 10a-b). Otherwise, it cannot be lowered due to the minimum pressure constraint (Fig. 10c). Therefore, binary zeotropic pairs with critical temperatures above 175 ℃ cannot benefit from the glide in the condenser (red region in Fig. 8b). On the other hand, azeotropic mixtures could also be beneficial. In minimum-boiling azeotropic mixtures, for some composition range, the boiling temperature of the mixture is lower than that of both its pure constituents (Fig. 3b). Therefore, the bubble temperature in the condenser becomes lower for some composition range (Fig. 10d) and the mixture generates more power compared to its pure constituents.

Fig. 11 represents the maximum glide for mixtures in minimum operating conditions. To better visualize the changes in maximum glide, glide values over 40 K are filtered out. Mixtures close to the diagonal line have close critical temperatures ($T_{c,1} \approx T_{c,2}$) and lower glide. It is also clear in Fig. 5 where near-azeotropic mixtures are located close to the

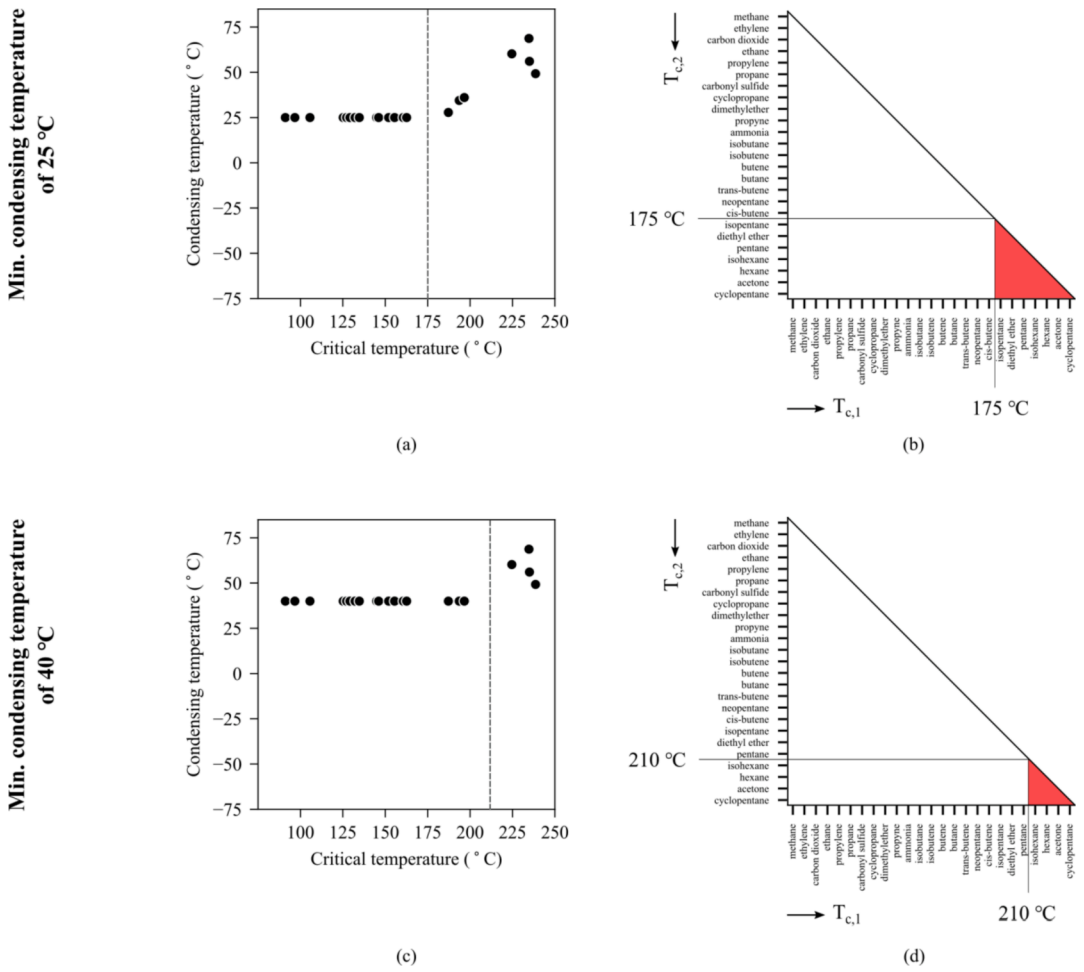


**Fig. 8.** (a-b) Minimum condensing temperature of 25 °C, (c-d): minimum condensing temperature of 40 °C, (a) condensing temperature vs. critical temperature of pure fluids at $T_{cond,min} = 25$ °C, (b) region division for binary mixtures at $T_{cond,min} = 25$ °C, based on condensing temperature (c) condensing temperature vs. critical temperature of pure fluids at $T_{cond,min} = 40$ °C, (d) region division for binary mixtures for $T_{cond,min} = 40$ °C based on condensing temperature. In Figs (a) and (b), the dashed line shows the border to divide the fluids. The fluids on the left side of the border, have condensing temperature equal to $T_{cond,\,min}$, while fluids on the right side of the border are constrained by minimum allowable pressure. Red regions in (b) and (c) represent mixtures where the pressure rule applies to both fluids ($T_{cond,\,min} < T_{b,1}, T_{b,2}$).

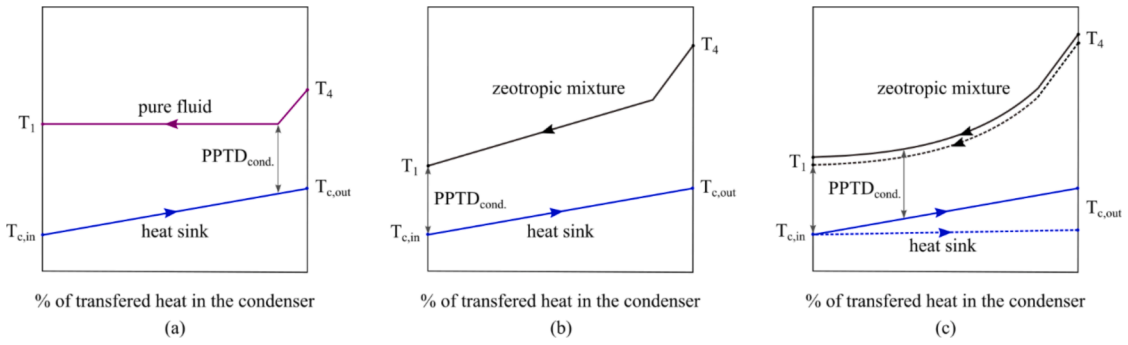


**Fig. 9.** Effect of glide condenser bubble temperature (a) pure fluid, (b) zeotropic mixture with minimum possible bubble temperature in condenser with pinch point at saturated liquid (c) zeotropic mixture with pinch point at 2-phase region.

diagonal line. On the other hand, mixtures with highest critical temperature difference ($T_{c,1} \ll T_{c,2}$) have highest glide which are located in lower left side of the table. Mixtures with high glide have high sensitivity to composition (steeper slope in glide-composition graphs as Fig. 4a). A slight change in composition will have significant effect on the performance of the cycle which makes these mixtures undesirable for Rankine cycle.

### 5.1.1. *Different fluid behaviors*

As explained in section 2, the effects of heat source on the cycle could be analyzed with effective heat source temperature. Cases with the same effective heat source temperature have the same trends in the behavior of net power and the same pinch point location in the evaporator.

Analyzing the behavior of fluids, 3 main behaviors were observed with regards to exergy efficiency (or net power) vs. evaporator pressure.

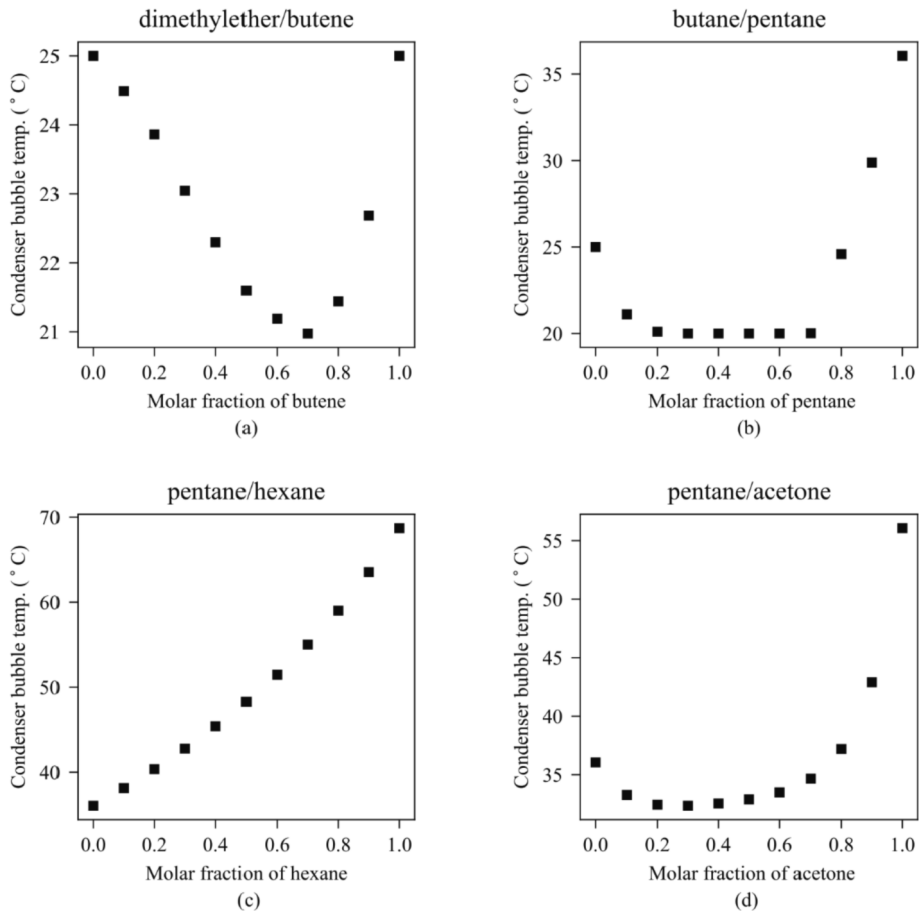


**Fig. 10.** Minimum bubble point in the condenser in different regions for zeotropic mixtures with $T_{cond,min} = 25$ °C and $\min\Delta T_c = 5$K (reference case) : (a):$T_{c,1}$ less than 175 °C, (b): $T_{c,1}$ less than 175 °C < $T_{c,2}$, (c):175 °C < $T_{c,1}$,$T_{c,2}$, (d): minimum boiling azeotropic mixture with 175 °C < $T_{c,1}$,$T_{c,2}$.

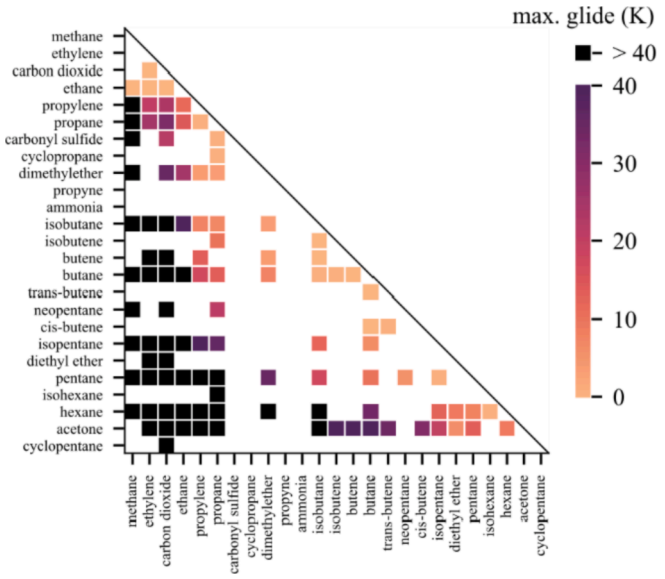


**Fig. 11.** Maximum glide for binary mixtures in condenser.

Fig. 12 shows 3 main categories for pentane with $T_c = 196.6$ °C. For $T_{h,eff} < 196.6$°C, the behavior is either descending or dome-shaped (type I). For 230 °C ≤ $T_{h,eff}$, the behavior is ascending with pressure (type III). For heat source temperatures in between 196.6 °C < $T_{h,eff}$ < 230°C, the behavior starts to change from dome-shaped to ascending.

The reason for these behaviors could be explained by the location of the pinch point in the evaporator and how the extracted exergy from the heat source varies by changing the evaporator pressure. Irreversibility distributions are presented for pentane at different heat source temperatures in Fig. 13. Increasing the evaporator pressure, results in less temperature difference between the fluid and heat source, decreasing the $\dot{I}_{evap.}$ (Fig. 13a-f). However, the behavior of $\dot{I}_h$ depends on the location of the pinch point in the evaporator. In pure fluids, for effective heat source temperature below critical temperature ($T_{h,eff} < T_c$), the pinch point in the evaporator occurs at saturated liquid and by increasing the evaporator pressure, the extracted heat in the evaporator decreases. The rate of increase of $\dot{I}_h$ is higher than the rate of decrease in $\dot{I}_{evap.}$ (Fig. 13a-b). Therefore, $\dot{I}_{tot.}$ increases, resulting in less exergy efficiency for high evaporator pressure in type I behavior (Fig. 12a-b and Fig. 13a-b).

If $T_c \ll T_{h,eff}$, the pinch point is located at the entrance of the evaporator, waste heat utilization is maximum (Fig. 13e-f) and consequently, net power will have a behavior like thermal efficiency, increasing with pressure (Eq. (7)) which explains the behavior of type III (Fig. 12e-f).

$$\dot{W}_{net} = \eta_{th} \times \dot{Q}_{evap} \tag{7}$$

For heat source temperature in between two previous cases (type II), the pinch point location varies between the evaporator inlet and the saturated liquid (Fig. 12c-d and Fig. 13c-d).

The behavior types of pure fluids present in Table 3 was investigated with different effective heat source temperatures. The results are displayed in Fig. 14 with different categories for the types of behaviors. These categories could be easily separated from each other.

The line $T_{h,eff} = 1.16T_C$ marks the border between type II and type

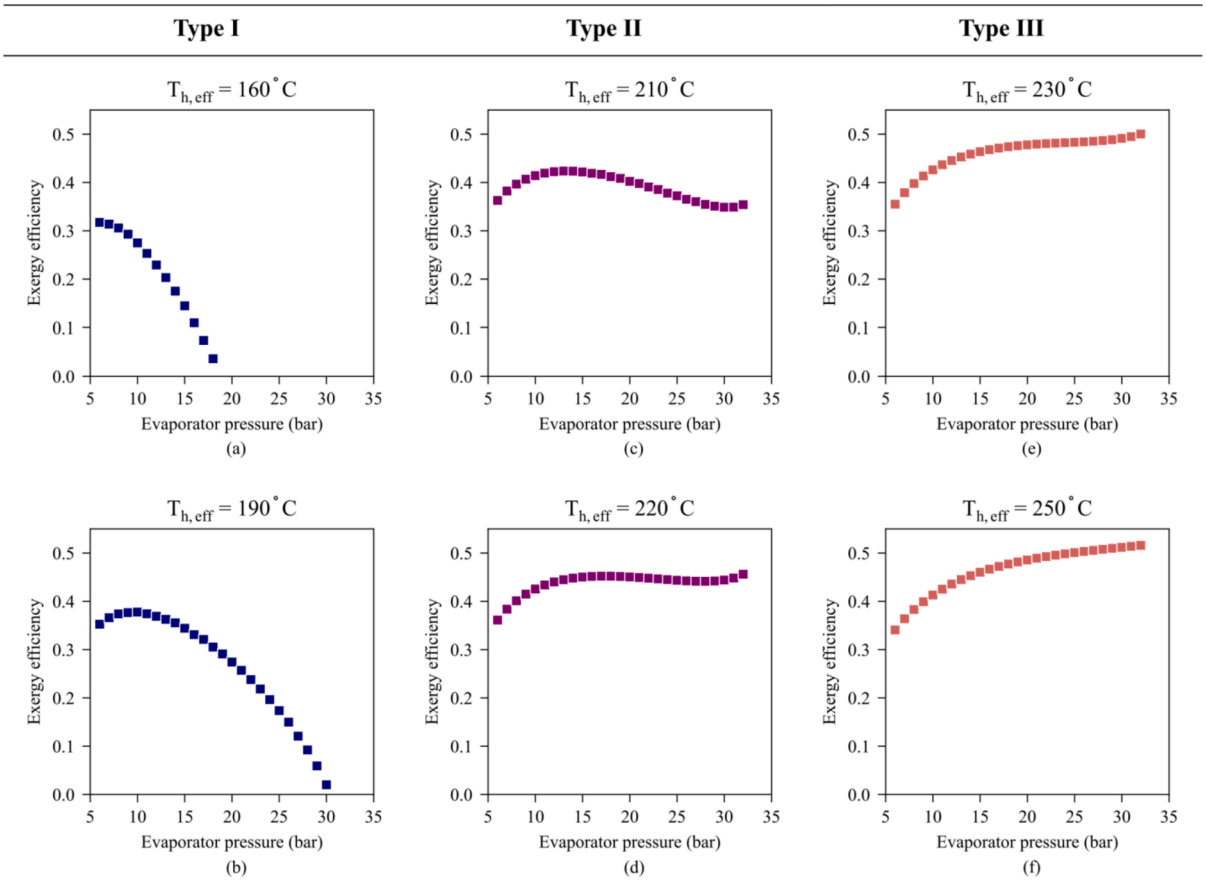


**Fig. 12.** Behavior type for pentane at different heat source temperatures ($T_c$ = 196.6 °C) showing exergy efficiency vs. evaporator pressure.

III, which is important in comparing the performance of a mixture with its pure constituents, discussed in section 5.2.1. The only misclassified point is acetone with $T_c$ = 235.0 °C at $T_{h,eff}$ = 265 °C which is predicted to be type II instead of type III.

For zeotropic mixtures, the same behavior is also observed. However, here the pinch point in the evaporator could also occur in 2-phase region. Analyzing the behavior of binary mixtures reveals that under the same conditions with regards to the heat source, heat sink and minimum PPTD, the mixture will behave similarly to its pure constituents. If both of the pure fluids belong to the same category, their mixture of any composition will have the same shape. If each of the fluids belongs to a different category, their mixture changes shape from one category towards another by varying composition. This is just regarding the trend behavior and not comparing the maximum performance of the mixture to pure fluids which will be dealt in section 5.2.1.

### 5.2. *Performance of binary zeotropic mixtures*

The performance of zeotropic mixtures could be studied within two perspectives:

- Comparing the performance of the mixture to its pure constituents
- Comparing the performance of the mixture to all the pure fluids (present in the study)

Both above comparisons are investigated in this paper. In this section, the results are presented mainly for the reference case while the differences between various cases are explained.

#### 5.2.1. *Comparing the performance of the mixture to its pure constituents*

In this comparison, different behaviors in mixtures are observed. Fig. 15 shows behavior examples of the mixtures compared to their own pure constituents for the reference case. Mixture curves are represented by their color based on molar fraction with intervals of 0.1. The performance of near-azeotropic mixture falls between the performance of its pure constituents regardless of the type of the fluids (type I, II, III in Fig. 12) (Fig. 15a-b). In another behavior type, the mixture outperforms both pure constituents in all pressure ranges (Fig. 15c-d). In other cases, the mixture outperforms the pure constituents just for a specific pressure range (Fig. 15e-f). In Fig. 15e the maximum exergy efficiency of the mixture is higher than that of both pure fluids. However, in Fig. 15f, the mixture could be interesting, if there exists a maximum allowable evaporator pressure. In all the other cases, the mixture does not provide any performance boost compared to pure fluids.

In order to study the behavior of the mixtures, we need to account for different sources of the irreversibility in the cycle. As explained in Eq. (2) and (4), there are 6 terms of irreversibility that contribute to the total irreversibility in the cycle. $\dot{I}_p$ and $\dot{I}_{exp.}$ are related to isentropic efficiencies of the pump and the expander. Although, they are taken into account, their share in the total irreversibility is low. The share of $\dot{I}_c$ is also low and its variation by mixture composition is small. Therefore, 3 main sources of irreversibility in the cycle are: $\dot{I}_h$, $\dot{I}_{evap.}$ and $\dot{I}_{cond.}$. Types of the fluids (type I, II, III in Fig. 12), glide in the condenser, normal boiling point of the fluids and the minimum condensing temperature affect how the main sources of the irreversibility change in mixtures compared to their pure constituents. $\dot{I}_{cond.}$ is an important factor considered in zeotropic mixtures to be minimized. $\dot{I}_{cond.}$ could be reduced for mixtures by lowering the bubble temperature. However, in the cases where the glide in the condenser is high, despite lower bubble temperature of the mixture in the condenser, dew temperature rises which results in higher $\dot{I}_{cond.}$ compared to its pure fluids. $\dot{I}_h$ depends on the behavior type of the

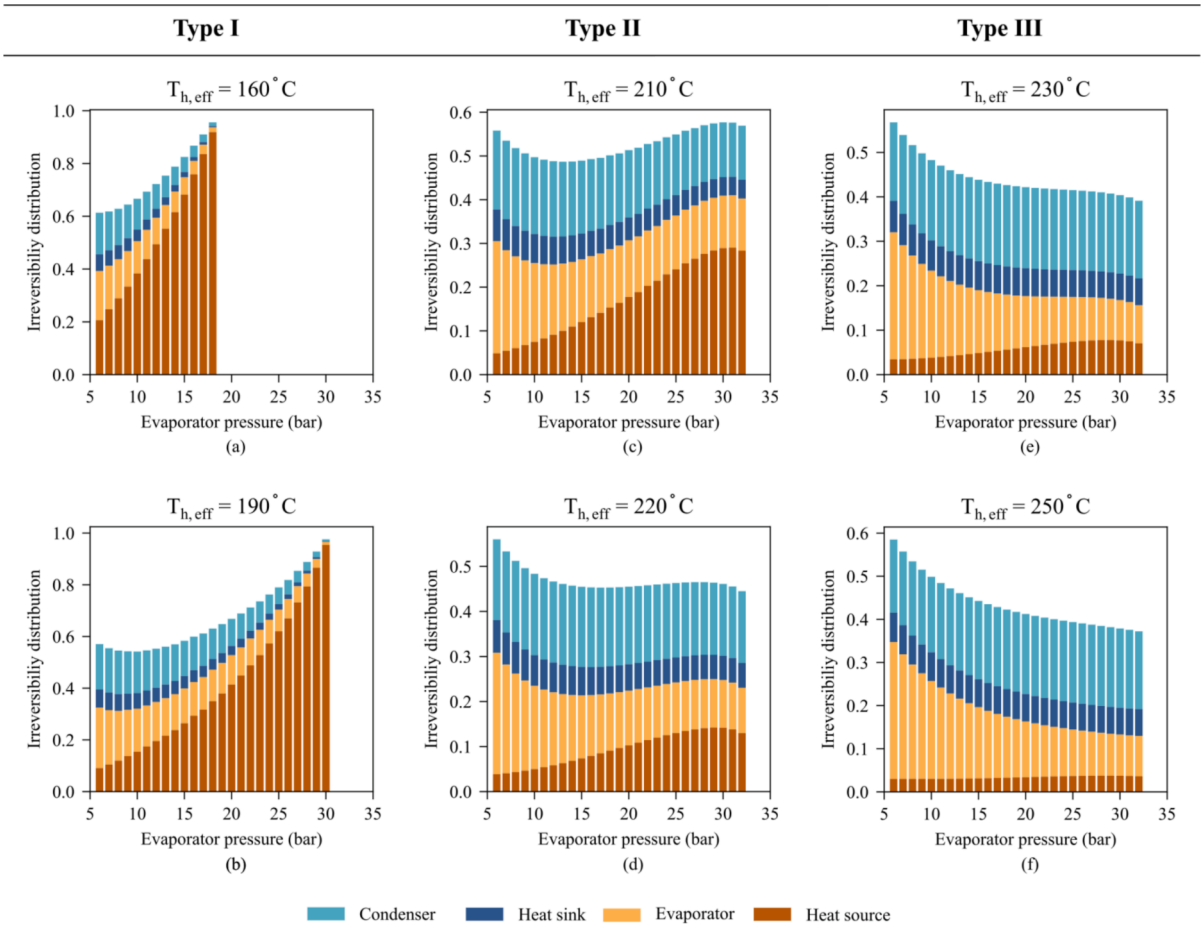


**Fig. 13.** Behavior type for pentane at different heat source temperatures ($T_c$ = 196.6 °C) showing irreversibility distribution vs. evaporator pressure.

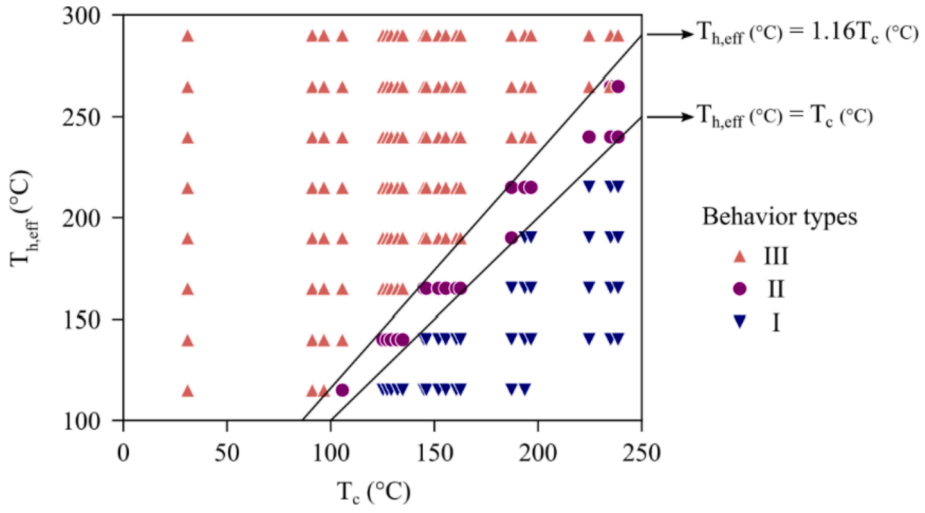


**Fig. 14.** $T_{h,eff}$ vs. $T_c$ and category type of behavior of pure fluids present in this study.

fluids and the bubble temperature of the mixtures in the condenser. In type III, the share of $\dot{I}_h$ is less than type I and as the location of the pinch point in the evaporator is at evaporator entrance, the lower bubble point results in less $\dot{I}_h$. For type I, the share of $\dot{I}_h$ is higher, due to the location of pinch point in the evaporator. $\dot{I}_{evap.}$ depends on the behavior type of the fluid. While mixing fluids of type III, the optimum point for each mixture composition is at the highest evaporator pressure. As the composition changes from the fluid with lower critical temperature to the fluid with higher critical temperature, $\dot{I}_{evap.}$ decreases. This is due to the less temperature difference between the heat source and the working fluid/mixture. In other cases, the behavior could be non-monotonic. Considering the variations in 3 main sources of the irreversibility, the performance of the mixture depends on the summation of all these factors. Reducing $\dot{I}_{cond.}$ does not necessarily guarantee performance improvement of the mixture, compared to its pure constituents.

In near-azeotropic mixtures, regardless of the behavior type of the

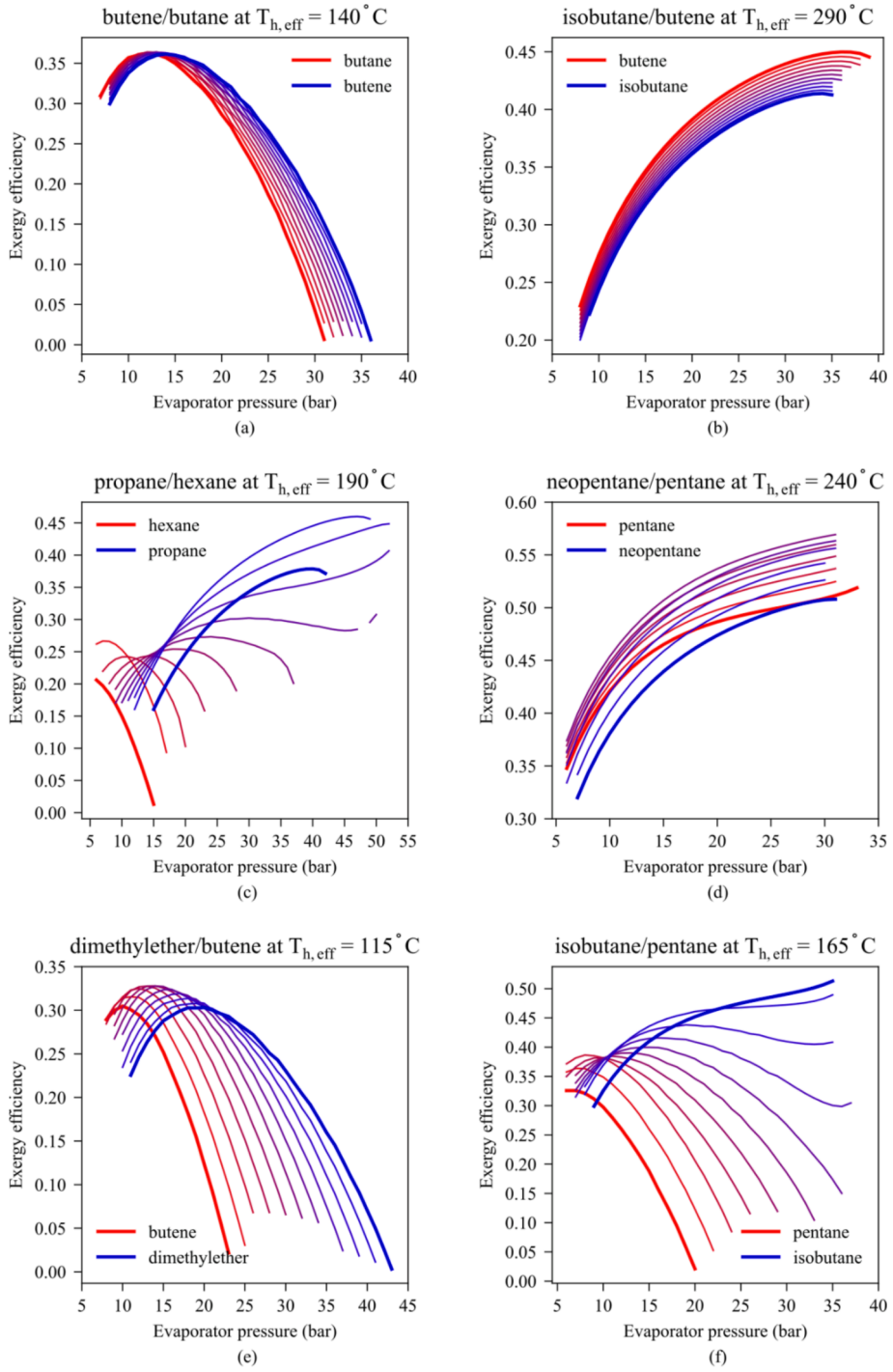


**Fig. 15.** Performance comparison of binary mixtures to pure constituents for the reference case. Mixtures are represented by their color based on molar fraction with intervals of 0.1.

fluids, the behavior of the mixture is not different from the behavior of its pure constituents. In this case the critical temperature of the fluids is close to each other and the glide in the condenser is less than 1 K. By changing the composition all the sources of irreversibility do not change, which results in the same performance of the mixture. The near-azeotropic mixtures are marked in Fig. 5.

In mixture of propane/hexane at $T_{h,eff.}$ = 190 °C, composition of (0.9/0.1) has higher exergy efficiency for all the evaporator pressure levels (Fig. 15c). Propane and hexane have type I and III behavior respectively. The maximum condenser glide is 70 K. For hexane, $\dot{I}_h$ is high and $\dot{I}_{evap.}$ low, while the opposite is true for propane. Although the bubble point in the condenser could be reduced, due to high glide, dew temperature in the mixture is higher than that of pure fluids, causing more temperature difference between temperature profiles in the condenser, resulting in higher $\dot{I}_{cond.}$. However, the summation of all these parameters decreases for mixture of (0.9 propane/0.1 hexane).

In mixture of neopentane/pentane at $T_{h,eff.}$ = 240°C, composition of (0.5/0.5) has the highest exergy efficiency (Fig. 15d). Both fluids have type III behavior. $\dot{I}_{evap.}$ decreases moving from pure neopentane to pure pentane. $\dot{I}_h$ is higher for pentane compared to neopentane due to higher condensing temperature. $\dot{I}_{cond.}$ is minimized at composition of (0.5/0.5). Considering all the sources of irreversibility, mixture of (0.5

neopentane/0.5 pentane) has highest performance.

In mixture of dimethylether/butene at $T_{h,eff.} = 115\ ^{\circ}C$, (Fig. 15e), $\dot{I}_{cond.}$ is minimized at composition of (0.4/0.6). The other sources of irreversibility change, but the overall performance of the cycle is maximized at this composition. However, the improvement is not significant compared to pure dimethylether and butene.

In mixture of isobutane/pentane at $T_{h.eff.} = 165^{\circ}C$ (Fig. 15f), $\dot{I}_{evap.}$ increases for mixtures, while $\dot{I}_{cond.}$ is minimized at the composition of (0.9/0.1). $\dot{I}_h$ has a non-monotonic behavior with minimum and maximum at pure isobutane and pentane, respectively. In overall performance, mixture does not boost exergy efficiency compared to its pure constituents.

Fig. 16 shows the relative increase percentage in the exergy efficiency of mixtures in comparison to their pure constituents, for different effective heat source temperatures for the reference case. Only the cases which improve the global performance of the pure fluids are considered and cases like Fig. 15f are not included. In this figure, azeotropic mixtures are excluded. As expected, near-azeotropic mixtures do not show any performance boost compared to their pure constituents.

In these graphs, the maximum exergy efficiency of the mixtures with minimum molar composition of 0.1 is compared to the maximum exergy efficiency of its pure constituents and heatmaps are presented as relative increase percentage in exergy efficiency for each specific effective heat source temperature. Black cells represent mixtures with relative increase in exergy efficiency of above 50%. These mixtures correspond to fluids with high critical temperature difference ($T_{c,1} \ll T_{c,2}$) at low effective heat source temperatures. Although the relative increase of exergy efficiency is high in these mixtures, the absolute value of the exergy efficiency is low. As the maximum relative increase in exergy efficiency changes in different cases, a specific colorbar is used for each case to better reveal the information on each mixture, compared to the other mixtures.

Analyzing the results in Fig. 16 reveals that the maximum relative

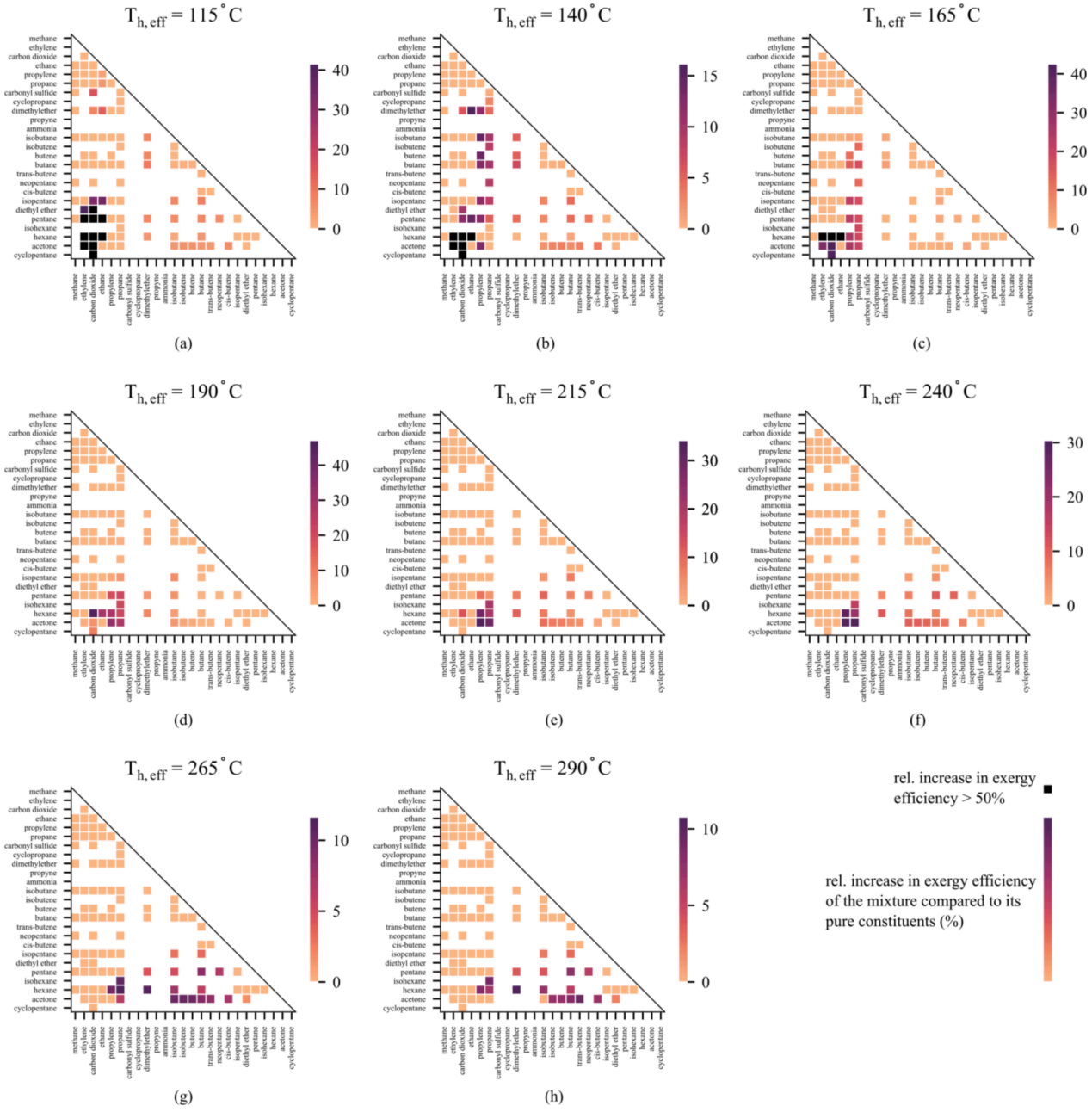


**Fig. 16.** Comparison of exergy efficiency of zeotropic mixtures to their pure constituents based on the relative increase in exergy efficiency for the reference case.

increase in exergy efficiency, decreases with heat source temperature. As in $T_{h,eff.} = 290$ °C, there is only a maximum of 10.76% relative increase in the exergy efficiency of the mixtures compared to their pure constituents. At each heat source temperature, the mixtures with the highest performance boost lie in lower left part of the table (high critical temperature difference) compared to the rest of the mixtures with boosted performance.

Next step was to map the mixtures which show performance boost compared to their pure constituents. It is very important not to draw very specific rules since, the information regarding some mixtures is missing due to non-availability of interaction parameters for those mixtures.

Results of zeotropic mixtures in Fig. 16 were categorized into 3 groups. Different categories include: mixtures with relative exergy efficiency boost $\geq$ 3%, mixtures with no performance boost or below 3%, and mixtures which have performance boost only in low pressure levels as Fig. 15f.

**Effect of minimum condensing temperature**

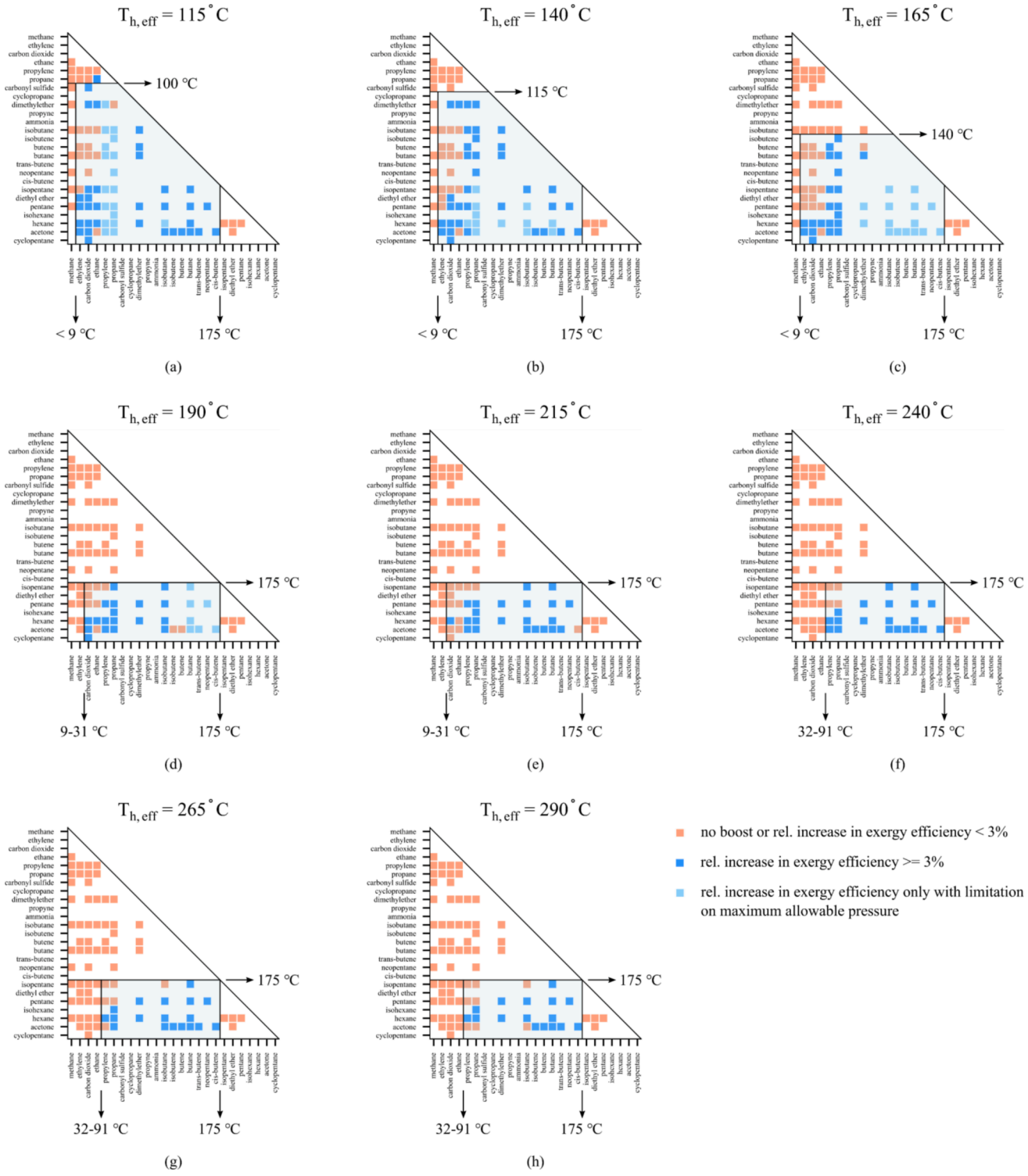


**Fig. 17.** Mapping of binary zeotropic mixtures where boosted mixtures compared to their pure constituents lie (Case 1: $T_{cond,min} = 25$ °C and $\min\Delta T_c = 5$K).

Fig. 17 and Fig. 18 represent the results for case 1 and case 2 respectively, where the minimum condensing temperature changes from 25 °C to 40 °C. Shaded blue regions represent the regions with mixtures which have boosted exergy efficiency above 3% or have exergy boost in low pressures. Not all the mixtures in this region outperform their pure constituents. Rather, the mixtures with boosted performance lie in that region with high probability. This region is controlled by 3 borders. The borders are identified as average critical temperature of the two neighboring fluids. In the cases where the difference between the critical temperature of the neighboring fluids is high, the range is written.

Naming horizontal axis $T_{c,1}$ (the fluid with lower critical temperature) and vertical axis as $T_{c,2}$ (the fluid with higher critical temperature), following generalized rules could be obtained based on minimum condensing temperature and effective heat source temperature presented in Table 4. Presenting the border which divides fluids based on the normal boiling point and minimum condensing conditions (borders in Fig. 8a and c) as $T_c^*$:

The mixture combination of fluids whose normal boiling point are higher than the minimum condensing temperature ($T_{cond,\,min} < T_{b,1}$, $T_{b,2}$, red region in (Fig. 8b and d) do not show any performance boost,

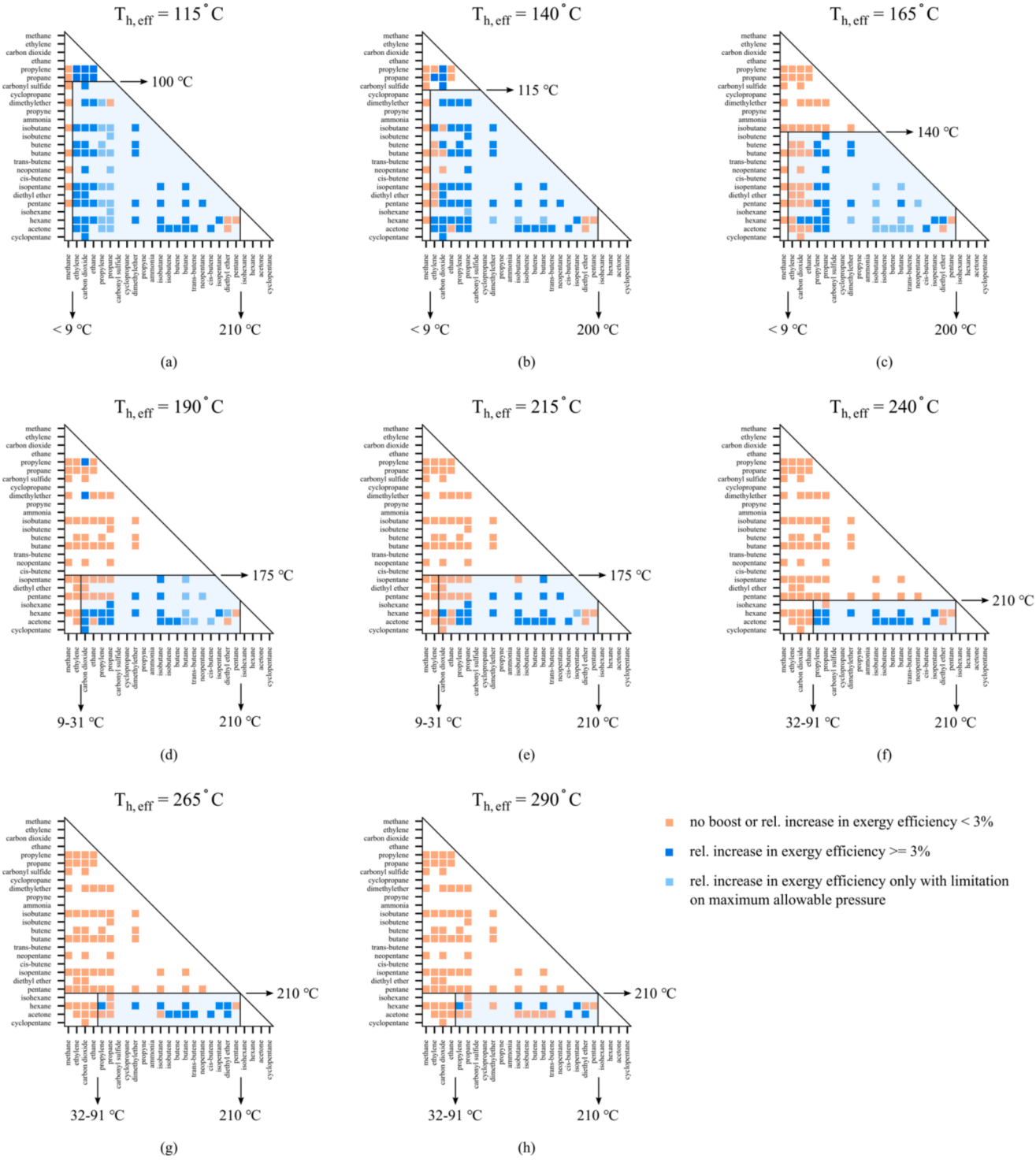


**Fig. 18.** Mapping of binary zeotropic mixtures where boosted mixtures compared to their pure constituents lie (Case 2: $T_{cond,min} = 40$ °C and $\min\Delta T_c = 5$K).

**Table 4**
Region rules for boosted performance of binary mixtures compared to their pure constituents [size: single column].

| Border | Rule | Critical temperature |
|---|---|---|
| right | Maximum of $T_{c,1}$ | $T_c^*$ |
| left | Minimum of $T_{c,1}$ | |
| top | Minimum of $T_{c,2}$ | Min ($T_c^*$, $T_{h,eff}/1.16$) |

which sets a maximum on $T_{c,1}$ equal to $T_c^*$. For the left border (minimum of $T_{c,1}$), a trend is observed that by increasing effective heat source temperature, this border increases. However, it is difficult to formulate this border as the difference between the critical temperatures of the neighboring fluids in that region is high. The upper border (minimum of $T_{c,2}$) is controlled by minimum of $T_c^*$ and the critical temperature at which the behavior type changes from type III to type II in.

Fig. 14 ($T_{h,eff}/1.16$). It means that a mixture combination of fluids with type III behavior does not improve the performance unless $T_{b,1} < T_{cond,\ min} < T_{b,2}$ as in Fig. 15d.

In low effective heat source temperatures of 115 °C and 140 °C, the prediction is not accurate. However, in the other cases, the region where boosted mixtures lie is predicted accurately, with high probability.

Therefore, both heat source and heat sink conditions control the minimum and the maximum critical temperature of the fluids whose binary mixture could have boosted performance compared to pure constituents. It is important to mention that these conclusions were based on the mixtures whose interaction parameters were available in REFPROP.

**Effect of minimum temperature rise in the heat sink**

Minimum temperature rise in the heat sink, accounts for how much the bubble temperature in the condenser could be lowered in mixtures, compared to pure fluids. This parameter affects how $\dot{I}_{cond.}$ changes in

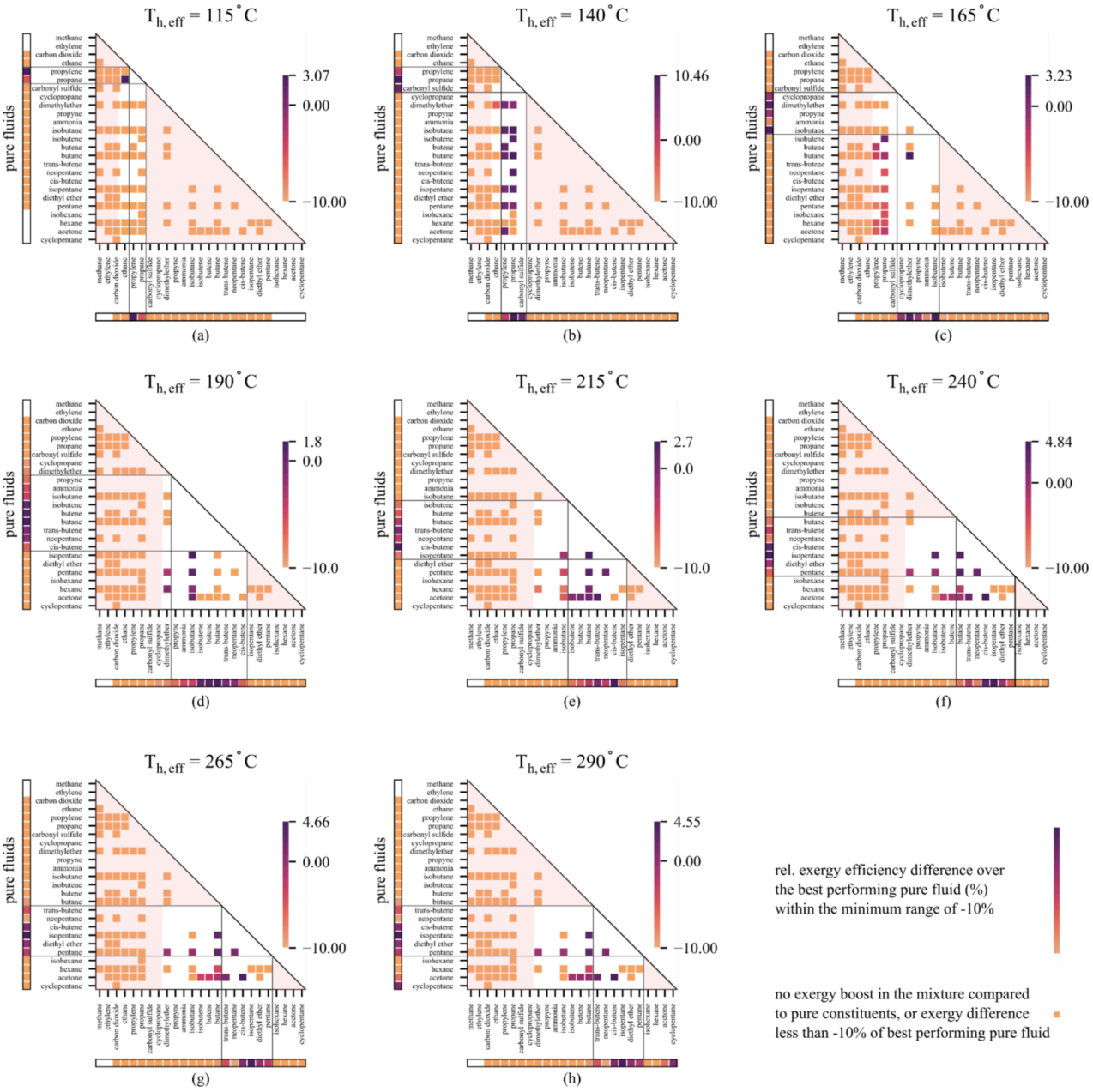


**Fig. 19.** Comparison of exergy efficiency of binary mixtures which outperform their pure constituents to all the pure fluids available in the study for different effective heat source temperatures, for the reference case.

mixtures compared to their pure constituents. Changing this parameter does not affect the general rules obtained in the previous section. However, the maximum performance boost over pure constituents, increases for some mixtures.

### 5.2.2. Comparing the performance of the mixture to all the pure fluids

In this section, the exergy efficiency values of the boosted mixtures are compared to the best performing pure fluid within each heat source to see if any binary mixture outperforms best pure fluids. Fig. 19 compares the exergy efficiency of boosted binary mixtures (which outperform their pure constituents by at least 3% relative) to the best performing pure fluid, for the reference case and the results are presented as the relative difference percentage compared to the best pure fluid. Only pure fluids and boosted zeotropic mixtures within the range of −10% of the best performing pure fluid are shown. All the other results are filtered out. The maximum boost comparing mixtures and pure fluids belongs to the effective heat source temperature of 140 ℃ with 10.46%. All the other cases of heat source temperature have performance boost of less than 5% compared to the best performing fluid.

At each heat source temperature, the critical temperature range of best performing pure fluids is mapped to the binary mixture table to compare where the best mixtures lie in the table compared to best pure fluids. Comparing the critical temperature range of best pure fluids to the best zeotropic mixtures, it is concluded that:

The combination of pure fluids, where the critical temperature of both fluids is below or above the range, are excluded. Besides, fluids whose critical temperature are 30 K less than the optimum critical temperature range should be excluded. These regions are marked with light red in Fig. 19. In all the cases, best performing pure fluids have critical temperature lower than the effective heat source temperatures which makes type I behaviors (in Fig. 12) not among the best performing pure fluids.

Applying the rules and including blue regions in section 5.2.1 and excluding red regions in section 5.2.2, it is possible to map the regions with performance boost compared to their pure constituents and high absolute exergy efficiency.

Table 5 presents exergy efficiency for the best pure fluid for each heat source temperature for reference case. Then pure fluids within the range of −10% of the pest pure fluid are presented with their relative percentage difference. Besides, mixtures with performance above the best pure fluid are shown with their relative boost in exergy efficiency compared to the best pure fluid. Many mixtures at.

**Table 5**
Exergy efficiency for the best pure fluid for each heat source temperature for reference case. Pure fluids within the range of −10% of the best pure fluid as well as mixtures with performance above the best pure fluid are presented with their relative percentage difference.

| $T_{h,eff}$ = 115 °C | | Best pure: propylene (39.5%) | | $T_{h,eff}$ = 140 °C | | Best pure: propane (44.0%) | |
|---|---|---|---|---|---|---|---|
| propane | −6.3% | ethane/propane | 3.1% | propylene | −4.9% | propylene/dimethylether | 6.2% |
| | | | | | | propylene/isobutane | 8.7% |
| | | | | | | propylene/butene | 8.1% |
| | | | | | | propylene/butane | 7.3% |
| | | | | | | propylene/isopentane | 6.3% |
| | | | | | | propylene/pentane | 6.7% |
| | | | | | | propylene/acetone | 7.3% |
| | | | | | | propane/ dimethylether | 4.9% |
| | | | | | | propane/isobutane | 10.3% |
| | | | | | | propane/isobutene | 8.7% |
| | | | | | | propane/butane | 10.5% |
| | | | | | | propane/neopentane | 9.1% |
| | | | | | | propane/isopentane | 8.6% |
| | | | | | | propane/pentane | 5.5% |
| $T_{h,eff}$ = 165 °C | | Best pure: isobutane (51.0%) | | $T_{h,eff}$ = 190 °C | | Best pure: butane (54.9%) | |
| cyclopropane | −3.3% | propane/isobutene | 1.4% | cyclopropane | −9.2% | isobutane/isopentane | 1.8% |
| dimethylether | −0.6% | dimethylether/butane | 3.2% | dimethyl ether | −8.5% | isobutane/pentane | 0.9% |
| propyne | −3.5% | | | propyne | −7.4% | | |
| isobutene | −9.8% | | | isobutane | −5.4% | | |
| | | | | isobutene | −0.9% | | |
| | | | | butene | −0.7% | | |
| | | | | *trans*-butene | −2.2% | | |
| | | | | neopentane | −2.5% | | |
| | | | | *cis*-butene | −6.7% | | |
| $T_{h,eff}$ = 215 °C | | Best pure: *cis*-butene (56.6%) | | $T_{h,eff}$ = 240 °C | | Best pure: isopentane (55.3%) | |
| isobutene | −7.7% | butane/pentane | 1.8% | butene | −10% | isobutane/isopentane | 3.5% |
| butene | −6.6% | butane/acetone | 0.9% | butane | −7.8% | butane/isopentane | 4.3% |
| butane | −4.4% | *trans*-butene/acetone | 2.2% | *trans*-butene | −4.7% | butane/pentane | 3.8% |
| *trans*-butene | −2.2% | neopentane/pentane | 1.4% | neopentane | −8.1% | *trans*-butene/acetone | 2.4% |
| neopentane | −4.9% | | | *cis*-butene | −0.9% | neopentane/pentane | 2.9% |
| isopentane | −7.8% | | | diethylether | −3.4% | *cis*-butene/acetone | 4.8% |
| | | | | pentane | −6.9% | | |
| $T_{h,eff}$ = 265 °C | | Best pure: isopentane (53.3%) | | $T_{h,eff}$ = 290 °C | | Best pure: isopentane (50.8%) | |
| butane | −9.1% | butane/isopentane | 3.4% | butane | −9.3% | butane/isopentane | 3.1% |
| *trans*-butene | −6.2% | butane/pentane | 3.5% | *trans*-butene | −6.3% | butane/acetone | 2.6% |
| neopentane | −9.6% | *trans*-butene/acetone | 1.7% | neopentane | −9.7% | neopentane/pentane | 1.4% |
| *cis*-butene | −2.4% | neopentane/pentane | 1.7% | *cis*-butene | −2.5% | *cis*-butene/acetone | 4.5% |
| diethyl ether | −3.4% | *cis*-butene/acetone | 4.7% | diethyl ether | −2.9% | | |
| pentane | −4.7% | | | pentane | −4.3% | | |
| | | | | acetone | −7.5% | | |
| | | | | cyclopentane | −2.4% | | |

### 5.3. Mixture screening method

The analyses results are briefed into screening criteria for mixtures:

**Step 1: Preparation of the triangular table with available fluids in the study, sorted by their critical temperature.** Table of fluids as presented in Fig. 5 should be prepared.

**Step 2: Removing the pairs where normal boiling point of both pure fluids is higher than the minimum condensing temperature for pure fluids.** Mixtures in this region cannot benefit from the glide in the condenser due to the minimum condensing pressure of 101.3 kPa. This rule could be translated as the maximum critical temperature of the fluids, discussed in section 5.1.1. A minimum condensing temperature of 25 °C (ambient temperature of 10 °C, cold region) sets a maximum critical temperature of 175°Cand a minimum condensing temperature of 40 °C (ambient temperature of 25 °C, hot region) sets a maximum critical temperature of 210 °C.

**Step 3: Applying minimum to the critical temperature of both pure fluids.** Based on the effective heat source temperature and condensing conditions in step 2, minimum temperature is applied to both fluids based on Table 4 and discussed in section 5.2.1. This region marks the mixture which could have boosted performance compared to their pure constituents.

**Step 4: Mapping the critical temperature range of the best pure fluids for the specific heat source temperature**. Mixtures where the critical temperature of both fluids is above or below this range should be excluded. Fluids with critical temperature of 30 K below the range should be also excluded, discussed in section 5.2.2. Rest of the mixtures represent mixtures which could have high absolute exergy efficiency.

**Step 5: Finding the intersection of regions in step 3 and 4.** The intersection of regions in step 3 and 4 represents potentially the mixtures with boost compared to their pure constituents and high absolute exergy efficiency.

**Step 6: Avoiding fluids with very high critical temperature difference.** Although mixtures of fluids with high critical temperature difference have high performance boost compared to their pure constituents, their absolute exergy efficiency is low. Besides, they have high condenser glide with high sensitivity toward composition. A slight change in the composition will have a high impact on the performance of the mixture in the cycle.

## 6. Conclusion

In this study, we analyzed all binary mixtures of natural fluids whose interaction parameter exists in REFPROP. The mixtures were investigated in subcritical cycles with heat source temperatures of 125–300 °C. Having glide, these mixtures could possibly enhance the performance of the cycle by decreasing the irreversibilities in the evaporator and the condenser. However, a glide does not guarantee performance boost. For this reason, we applied a thermodynamic model to predict the performance of the ORC considering binary mixtures and their pure components for different heat source cases.

Binary mixtures were investigated within two frameworks: comparing the mixture to its pure constituents and best performing pure fluid. In the first perspective, it was possible to draw few rules to map the binary mixtures with boosted performance compared to their pure constituents. These rules are based on the heat source, heat sink, normal boiling point and minimum condensing temperature for pure fluids. This improvement decreases with heat source temperature, as at $T_{h,eff}$=°C, only a maximum of 10.76% improvement is observed for a binary mixture compared to its pure constituents for the reference case. In the second perspective, results show a maximum of 10% improvement to the best performing fluid at $T_{h,eff} = 140$ °C, while in other heat source temperatures, the improvement is below 5%.

Maximum allowable pressure in the evaporator also plays an important role whether a mixture is superior to its pure constituents or not. A mixture with a fixed composition which has a fixed critical temperature and condenser glide, could behave differently at different evaporator pressure levels.

In the second perspective, mixtures which have boosted performance compared to their pure constituents and have high exergy efficiency were identified. First the optimum critical temperature range of pure fluids was found for each heat source temperature. Then binary pairs of fluids whose critical temperatures are both above or below the range were excluded. Fluids with critical temperature of 30 K below the optimum range were also excluded.

Finally, a screening method is presented to map the binary mixtures with performance boost compared to pure constituents and high absolute exergy efficiency.

This study is helpful for future in-depth studies, where it is desirable to minimize the number of candidate binary mixtures for further investigation as well as multi-component mixtures.

### CRediT authorship contribution statement

**Mina Shahrooz:** Conceptualization, Methodology, Visualization, Investigation, Software, Writing – original draft. **Per Lundqvist:** Conceptualization, Writing – review & editing. **Petter Nekså:** Writing – review & editing.

### Declaration of Competing Interest

The authors declare that they have no known competing financial interests or personal relationships that could have appeared to influence the work reported in this paper.

### Acknowledgement

This work has been funded by HighEFF - Center for an Energy Efficient and Competitive Industry for the Future, an 8-year Research Center under the FME-scheme (Center for Environment-friendly Energy Research, 257632/E20). The authors gratefully acknowledge the financial support from the Research Council of Norway and user partners of HighEFF.

### References

[1] Liao G, E J, Zhang F, Chen J, Leng E. Advanced exergy analysis for Organic Rankine Cycle-based layout to recover waste heat of flue gas. Appl Energy 2020;266:114891.
[2] Wei D, Lu X, Lu Z, Gu J. Performance analysis and optimization of organic Rankine cycle (ORC) for waste heat recovery. Energy Convers Manag 2007;48(4):1113–9. https://doi.org/10.1016/j.enconman.2006.10.020.
[3] Behzadi A, Gholamian E, Houshfar E, Habibollahzade A. Multi-objective optimization and exergoeconomic analysis of waste heat recovery from Tehran's waste-to-energy plant integrated with an ORC unit. Energy 2018;160:1055–68. https://doi.org/10.1016/j.energy.2018.07.074.
[4] Noriega Sanchez CJ, Gosselin L, da Silva AK. Designed binary mixtures for subcritical organic Rankine cycles based on multiobjective optimization. *Energy Convers Manag* 2018;156(November 2017):585–96. https://doi.org/10.1016/j.enconman.2017.11.050.
[5] Xu W, Zhao L, Mao SS, Deng S. Towards novel low temperature thermodynamic cycle: a critical review originated from organic Rankine cycle. Appl Energy 2020;270:115186.
[6] Aljundi IH. Effect of dry hydrocarbons and critical point temperature on the efficiencies of organic Rankine cycle. Renew Energy 2011;36(4):1196–202. https://doi.org/10.1016/j.renene.2010.09.022.
[7] Mago PJ. Exergetic evaluation of an organic rankine cycle using medium-grade waste heat. Energy Sourc Part A Recover Util Environ Eff 2012;34(19):1768–80. https://doi.org/10.1080/15567036.2010.492382.
[8] Hærvig J, Sørensen K, Condra TJ. Guidelines for optimal selection of working fluid for an organic Rankine cycle in relation to waste heat recovery. Energy 2016;96:592–602. https://doi.org/10.1016/j.energy.2015.12.098.
[9] Xu J, Yu C. Critical temperature criterion for selection of working fluids for subcritical pressure Organic Rankine cycles. Energy 2014;74(C):719–33. https://doi.org/10.1016/j.energy.2014.07.038.
[10] Zhai H, An Q, Shi L. Analysis of the quantitative correlation between the heat source temperature and the critical temperature of the optimal pure working fluid for subcritical organic Rankine cycles. Appl Therm Eng 2016;99:383–91. https://doi.org/10.1016/j.applthermaleng.2016.01.058.

[11] Yang L, Gong M, Guo H, Dong X, Shen J, Wu J. Effects of critical and boiling temperatures on system performance and fluid selection indicator for low temperature organic Rankine cycles. Energy 2016;109:830–44. https://doi.org/10.1016/j.energy.2016.05.021.

[12] Ayachi F, Boulawz Ksayer E, Zoughaib A, Neveu P. ORC optimization for medium grade heat recovery. Energy 2014;68:47–56. https://doi.org/10.1016/j.energy.2014.01.066.

[13] Zhao J, Hu L, Wang Y, Yin H, Deng S, Li W, et al. How to rapidly predict the performance of ORC: Optimal empirical correlation based on cycle separation. Energy Convers Manag 2019;188:86–93.

[14] Wang Y, Zhao J, Chen G, Deng S, An Q, Luo C, et al. A new understanding on thermal efficiency of organic Rankine cycle: Cycle separation based on working fluids properties. Energy Convers Manag 2018;157:169–75.

[15] Chen G, An Q, Wang Y, Zhao J, Chang N, Alvi J. Performance prediction and working fluids selection for organic Rankine cycle under reduced temperature. *Appl Therm Eng* 2019;153(April 2018):95–103. https://doi.org/10.1016/j.applthermaleng.2019.02.011.

[16] Barse KA, Mann MD. Maximizing ORC performance with optimal match of working fluid with system design. Appl Therm Eng 2016;100:11–9. https://doi.org/10.1016/j.applthermaleng.2016.01.167.

[17] Lecompte S, Huisseune H, van den Broek M, Vanslambrouck B, De Paepe M. Review of organic Rankine cycle (ORC) architectures for waste heat recovery. Renew Sustain Energy Rev 2015;47:448–61. https://doi.org/10.1016/j.rser.2015.03.089.

[18] Miao Z, Zhang K, Wang M, Xu J. Thermodynamic selection criteria of zeotropic mixtures for subcritical organic Rankine cycle. Energy 2019;167:484–97. https://doi.org/10.1016/j.energy.2018.11.002.

[19] Collings P, Yu Z, Wang E. A dynamic organic Rankine cycle using a zeotropic mixture as the working fluid with composition tuning to match changing ambient conditions. Appl Energy 2016;171:581–91. https://doi.org/10.1016/j.apenergy.2016.03.014.

[20] Li J, Ge Z, Duan Y, Yang Z. Effects of heat source temperature and mixture composition on the combined superiority of dual-pressure evaporation organic Rankine cycle and zeotropic mixtures. Energy 2019;174:436–49. https://doi.org/10.1016/j.energy.2019.02.186.

[21] Cao X, Zhang CL, Zhang ZY. Cycle à plusieurs niveaux de pression-Une nouvelle approche du cycle de Lorenz. Int J Refrig 2017;74:281–92. https://doi.org/10.1016/j.ijrefrig.2016.10.017.

[22] Lecompte S, Ameel B, Ziviani D, Van Den Broek M, De Paepe M. Exergy analysis of zeotropic mixtures as working fluids in Organic Rankine Cycles. Energy Convers Manag 2014;85:727–39. https://doi.org/10.1016/j.enconman.2014.02.028.

[23] Deethayat T, Asanakham A, Kiatsiriroat T. Performance analysis of low temperature organic Rankine cycle with zeotropic refrigerant by Figure of Merit (FOM). Energy 2016;96:96–102. https://doi.org/10.1016/j.energy.2015.12.047.

[24] Lu P, et al. Thermo-economic design, optimization, and evaluation of a novel zeotropic ORC with mixture composition adjustment during operation. *Energy Convers Manag* 2021;230:113771. https://doi.org/10.1016/j.enconman.2020.113771.

[25] Lu J, Zhang J, Chen S, Pu Y. Analysis of organic Rankine cycles using zeotropic mixtures as working fluids under different restrictive conditions. Energy Convers Manag 2016;126:704–16. https://doi.org/10.1016/j.enconman.2016.08.056.

[26] Modi A, Haglind F. A review of recent research on the use of zeotropic mixtures in power generation systems. Energy Convers Manag 2017;138:603–26. https://doi.org/10.1016/j.enconman.2017.02.032.

[27] Zhou Y, Zhang F, Yu L. Performance analysis of the partial evaporating organic Rankine cycle (PEORC) using zeotropic mixtures. Energy Convers Manag 2016;129:89–99. https://doi.org/10.1016/j.enconman.2016.10.009.

[28] Miao Z, Zhang K, Wang M, Xu J. Thermodynamic selection criteria of zeotropic mixtures for subcritical organic Rankine cycle. Energy 2019;167:484–97. https://doi.org/10.1016/j.energy.2018.11.002.

[29] Zühlsdorf B, Jensen JK, Cignitti S, Madsen C, Elmegaard B. Analysis of temperature glide matching of heat pumps with zeotropic working fluid mixtures for different temperature glides. Energy 2018;153:650–60. https://doi.org/10.1016/j.energy.2018.04.048.

[30] Mondejar ME, Thern M. Analysis of isentropic mixtures for their use as working fluids in organic Rankine cycles. Environ Prog Sustain Energy 2017;36(3):921–35. https://doi.org/10.1002/ep.12520.

[31] Shahrooz M, Lundqvist P, Nekså P. Effect of Working Fluid Type on Low Temperature Rankine, no. September, pp. 1–8, 2019, [Online]. Available: https://www.researchgate.net/publication/335857810_Effect_of_Working_Fluid_Type_on_Low_Temperature_Rankine_Cycle_Optimization.

[32] Kiva VN, Hilmen EK, Skogestad S. Azeotropic phase equilibrium diagrams: a survey. Chem Eng Sci 2003;58(10):1903–53. https://doi.org/10.1016/S0009-2509(03)00018-6.

[33] Bevanott J, Boeriogoates J. Applications of thermodynamics to phase equilibria studies of mixtures. Chem Thermodyn Adv Appl 2000;4:115–59. https://doi.org/10.1016/b978-012530985-1/50005-9.

[34] Privat R, Jaubert JN. Classification of global fluid-phase equilibrium behaviors in binary systems. Chem Eng Res Des 2013;91(10):1807–39. https://doi.org/10.1016/j.cherd.2013.06.026.

[35] Hadler AB, Ott LS, Bruno TJ. Study of azeotropic mixtures with the advanced distillation curve approach. Fluid Phase Equilib 2009;281(1):49–59. https://doi.org/10.1016/j.fluid.2009.04.001.

[36] Liang S, Cao Y, Liu X, Li X, Zhao Y, Wang Y, et al. Insight into pressure-swing distillation from azeotropic phenomenon to dynamic control. Chem Eng Res Des 2017;117:318–35.

[37] Aucejo A, Montón JB, Muñoz R, Wisniak J. Double azeotropy in the benzene + hexafluorobenzene system. J Chem Eng Data 1996;41(1):21–4. https://doi.org/10.1021/je9501346.

[38] Lv L, Li H, Zhang Z, Huang H. Comparison of the economy and controllability of pressure swing distillation with two energy-saving modes for separating a binary azeotrope containing lower alcohols. *Processes* 2019;7(10). https://doi.org/10.3390/pr7100730.

[39] E.W. Lemmon, I.H. Bell, M.L. Huber, M.O. McLinden. "NIST Standard Reference Database 23: Reference Fluid Thermodynamic and Transport Properties-REFPROP, Version 10.0, National Institute of Standards and Technology." 2018, Accessed: Sep. 02, 2021. [Online]. Available: https://pages.nist.gov/REFPROP-docs/.

[40] Harris CR, Millman KJ, van der Walt SJ, Gommers R, Virtanen P, Cournapeau D, et al. Array programming with NumPy. Nature 2020;585(7825):357–62.

[41] McKinney W. Data structures for statistical computing in python. In: in *In Proceedings of the 9th Python in Science Conference*; 2010. p. 51–6.

[42] Virtanen P, Gommers R, Oliphant TE, Haberland M, Reddy T, Cournapeau D, et al. SciPy 1.0: fundamental algorithms for scientific computing in Python. Nat Methods 2020;17(3):261–72.

[43] Hunter JD. MATPLOTLIB: A 2D GRAPHICS ENVIRONMENT. Comput Sci Eng 2007;9(3):90–5.

[44] Waskom M. Seaborn: statistical data visualization. J Open Source Softw 2021;6(60):3021. https://doi.org/10.21105/joss.03021.

[45] Shahrooz M, Lundqvist P, Nekså P. Natural refrigerants for low temperature power cycles. Refrig Sci Technol 2018;2018:1373–80. https://doi.org/10.18462/iir.gl.2018.1401.

[46] NguyenHuynh D, Mai CTQ, Tran STK, Nguyen XTT, Baudouin O. Modelling of phase behavior of ammonia and its mixtures using the mg-SAFT. Fluid Phase Equilib 2020;523:112689. https://doi.org/10.1016/J.FLUID.2020.112689.

[47] Xu X, Chen H, Liu C, Dang C. Prediction of the binary interaction parameter of carbon dioxide/alkanes mixtures in the pseudocritical region. ACS Omega 2019;4(8):13279–94. https://doi.org/10.1021/acsomega.9b01450.

[48] Bell IH, Lemmon EW. Automatic fitting of binary interaction parameters for multi-fluid Helmholtz-energy-explicit mixture models. J Chem Eng Data 2016;61(11):3752–60.

[49] Wang Y, Liu X, Ding X, Weng Y. Experimental investigation on the performance of ORC power system using zeotropic mixture R601a/R600a. Int J Energy Res 2017;41(5):673–88. https://doi.org/10.1002/ER.3664.

[50] Varshni YP. Critical temperatures of organic compounds from their boiling points. Phys Chem Liq 2009;47(4):383–98. https://doi.org/10.1080/00319100801889522.

[51] Kim KH, Ko HJ, Kim K. Assessment of pinch point characteristics in heat exchangers and condensers of ammonia-water based power cycles. Appl Energy 2014;113:970–81. https://doi.org/10.1016/J.APENERGY.2013.08.055.